COMPUTATIONAL MODELING OF FIN-AND-TUBE TYPE VEHICLE RADIATORS BASED ON POROUS MEDIUM APPROACH

A THESIS SUBMITTED TO
THE GRADUATE SCHOOL OF NATURAL AND APPLIED SICENCES
OF
MIDDLE EAST TECHNICAL UNIVERSTIY

BY

KADİR GÖKHAN GÜLER

IN PARTIAL FULLFILMENT OF THE REQUIREMENTS
FOR
THE DEGREE OF MASTER OF SCIENCE
IN
MECHANICAL ENGINEERING

MAY 2014

Approval of the thesis:

COMPUTATIONAL MODELING OF FIN-AND-TUBE TYPE VEHICLE RADIATORS BASED ON POROUS MEDIUM APPROACH

Submitted by **KADİR GÖKHAN GÜLER** in partial fulfillment of the requirements for the degree of **Masters of Science in Mechanical Engineering Department, Middle East Technical University** by,

Prof. Dr. Canan Özgen
Dean, Graduate School of **Natural and Applied Sciences** _____

Prof. Dr. Süha Oral
Head of Department, **Mechanical Engineering** _____

Prof. Dr. M. Haluk Aksel
Supervisor, **Mechanical Engineering Dept., METU** _____

Assist. Prof. Dr. Barbaros Çetin
Co-supervisor, **Mech. Eng. Dept., İhsan Doğramacı Bilkent Uni.** _____

Examining Committee Members:

Prof. Dr. Kahraman Albayrak
Mechanical Engineering Dept., METU _____

Prof. Dr. M. Haluk Aksel
Mechanical Engineering Dept., METU _____

Assist. Prof. Dr. Barbaros Çetin
Mech. Eng. Dept., İhsan Doğramacı Bilkent Uni. _____

Prof. Dr. Zafer Dursunkaya
Mechanical Engineering Dept., METU _____

Assoc. Prof. Dr. Ahmet Yozgatlıgil
Mechanical Engineering Dept., METU _____

Date: **29.05.2014**

I hereby declare that all information in this document has been obtained and presented in accordance with academic rules and ethical conduct. I also declare that, as required by these rules and conduct, I have fully cited and referenced all material and results that are not original to this work.

Name, Last Name: KADİR GÖKHAN GÜLER

Signature :

ABSTRACT

COMPUTATIONAL MODELING OF FIN-AND-TUBE TYPE VEHICLE RADIATORS BASED ON POROUS MEDIUM APPROACH

Güler, Kadir Gökhan

M.S., Department of Mechanical Engineering

Supervisor : Prof. Dr. M. Haluk Aksel

Co-Supervisor : Assist. Prof. Dr. Barbaros Çetin

May 2014, 59 pages

A common tool for the determination of the thermal characteristics of fin-and-tube heat exchangers is the experimental testing. However, experimental testing is not feasible considering the cost and the labor-time. One alternative to the experimental testing is the utilization of computational fluid dynamics (CFD) analysis to predict the thermal characteristics of these kinds of radiators. However, CFD models are also not suitable to be used as a design tool since the considerably amount of computational power and the computational time required due to the complex geometric structures of the fins. This issue becomes problematic when the large-scale heavy-duty radiators are considered. Computational thermal performance analysis based on porous medium approach of a vehicle radiator is studied in this M.Sc. thesis. Fin side of the radiator is modeled as porous medium. Fluid flow and heat transfer characteristics are extracted from the unit cell fin domains and implementation is made into complete radiator assembly. Forchiemmer model is used for the porous medium characterization. Utilization of this modeling leads the way to obtain thermal and hydrodynamic characteristics of fin-tube type vehicle radiators.

Keywords: Porous media, fin-tube heat exchanger, computational fluid dynamics, vehicle radiator, thermal performance

ÖZ

GÖZENEKLİ ORTAM YAKLAŞIMI İLE FİN VE TÜP TİPİ ARAÇ RADYATÖRÜ SAYISAL MODELLEMESİ

Güler, Kadir Gökhan
Yüksek Lisans, Makine Mühendisliği bölümü
Tez Yöneticisi : Prof. Dr. M. Haluk Aksel
Ortak Tez Yöneticisi : Yard. Doç. Dr. Barbaros Çetin

Mayıs 2014, 59 sayfa

Günümüz teknolojisinde fin-tüp tipi ısı değiştiricilerin termal performanslarının çıkarımı deneysel çalışmalar ile elde edilmektedir. Deneysel çalışmalar, maliyet açısından ve deneylerin gerçekleştirilme süreleri açısından pratik uygulamalar için dezavantaj yaratmaktadır. Deneysel çalışmalara alternatif olarak termal performans çıkarımı hesaplamalı akışkanlar dinamiği (HAD) nümerik analiz yöntemi ile elde edilebilmektedir. Ancak fin-tüp tipi ısı değiştirici modellerinde fin yapısının tekrar eden ve karmaşık geometrisi sebebinden dolayı yüksek hesaplama gücü gerektirmektedir. Isı değiştiricinin fin kısmını gözenekli ortam yaklaşımı ile modellenmesi yüksek hesaplama gereksinimini oldukça düşürmektedir. Bu sayede tam ölçekli bir radyatör HAD modellemesi gerçekleştirilebilmektedir. Bu tezde gözenekli ortam yaklaşımı ile fin ve tüp tipi araç radyatörü sayısal modellemesi çalışması gerçekleştirilmiştir. Birim hücre fin simülasyonlarından, gözenekli ortam fin akış ve ısı transferi parametreleri elde edilerek tam ölçekli radyatör modellemesine uygulanmıştır. Gözenekli ortam modellemesi için Forcheimer yaklaşımı kullanılmıştır. Bu çalışmada geliştirilen yöntem ile fin-tüp tipi araç radyatörlerinin termal ve hidrodinamik karakterleri elde edilebilmektedir.

Anahtar Kelimeler: Gözenekli ortam, fin-tüp ısı değiştirici, hesaplamalı akışkanlar dinamiği, araç radyatörü

To humanity, if still exists …

ACKNOWLEGDEMENTS

I would like to express my deepest gratitude to my supervisor Prof. Dr. M. Haluk Aksel and co-supervisor Assist. Prof. Dr. Barbaros Çetin for their guidance, advice, criticism, encouragements and insight throughout the research.

Especially, I owe my sincere gratitude for my father, mother and my sister for their support all through my life.

TABLE OF CONTENTS

LIST OF TABLES

TABLES

LIST OF FIGURES

FIGURES

LIST OF ABBREVIATIONS

A	Flow Area
A_{fs}	Interfacial Area Density
$\overrightarrow{B_f}$	Body force
C_F	Dimensionless Form-Drag Constant
C_p	Specific Heat
C_2	Inertial Coefficient
E_f	Total Fluid Energy
E_s	Total Solid Medium Energy
$\vec{F}$	External Body Force
$\vec{g}$	Gravitational Acceleration
h	Sensible Enthalpy
h_{fs}	Heat Transfer Coefficient for Fluid/Solid Interface
I	Unit Tensor
$\vec{J}_j$	Diffusion Flux
k_f	Fluid Phase Thermal Conductivity
k_{eff}	Effective Conductivity
k_s	Solid Thermal Conductivity
L	Characteristic Length
$\dot{m}$	Mass Flow Rate
S_h	Heat Source
t	Fin Thickness
T_{ref}	Reference Temperature
T_w	Wall Temperature
Q	Heat Capacity
U	Free Stream Velocity
V	Average Velocity
μ	Dynamic Viscosity
$\tilde{\mu}$	Effective Viscosity
γ	Porosity
ρ	Density
α	Permeability
$\bar{\bar{\tau}}$	Stress Tensor
δ_d	Displacement Thickness
Δp	Pressure Drop
ΔT	Temperature Drop

CHAPTER 1

INTRODUCTION

During the conversion of fuel energy to mechanical energy by combustion, for casual engines approximately one-third of the energy goes to mechanical energy, one-third goes to exhaust heat and one-third goes to cooling system heat load [1]. In today's world, leading automotive companies are manufacturing more powerful and efficient engines. As the engines become more powerful, the energy created by the engine is increases and so does the heat load of the engine. Together with the increase in the heat load, the required cooling capacity of a radiator also increases [1]. Engine manufacturers specify the required cooling capacity according to their engine design parameters. For this reason, in general cooling capacity is a known input quantity. In addition to this, automotive companies also specify the fundamental size limitations of the required cooling system. An appropriate cooling system which fulfills the engine cooling capacity needs to be designed according to the specified input parameters.

The main component of a cooling system of an engine is a radiator. Radiators are typically fin-tube type heat exchangers. Radiators are composed of up-tank, low-tank, up and low trays, tubes and fins [1]. Simply, a radiator works with two fluids that are air and anti-freeze water mixture (which is defined in the literature as ethylene glycol (EG)) [1]. EG enters from the inlet of the radiator, passes through pipes, and exits through the outlet. When EG passes though the pipes, heat transfer occurs between two fluids, and the temperature of EG decreases. On the other side, cold air passes through the fins, and is heated up by the heat transferred from the EG [1]. A typical vehicle radiator is presented in Figure 1.

Figure 1.1: 4-row Tractor Radiator Produced by YETSAN Auto Radiator Co. Inc.

Cooling capacity of a radiator depends on the inlet mass flow rate of EG, inlet velocity of the air, the number of the tubes, sizing of the tubes, type of the fins, number of the fins, and the shape and location of the inlet and outlet manifolds. In a practical application, the design of an optimized radiator with respect to the cooling requirements of an engine is currently a challenging process. Major design criterion is the thermal performance besides the mechanical design parameters. Predicting the thermal performance of a radiator is a challenging issue. The heat capacity of a radiator can be acquired through experiment setups such as calorimeter testing or air-to-boil tests. However, the aforementioned experimental tests are expensive and time consuming. Moreover, when the optimization of a radiator is considered, even for a single radiator, these tests may be required repeatedly which makes experimentation even more time consuming and costly. Besides the experimental techniques, numerical methods such as the computational fluid dynamics (CFD) analysis can be used as a design tool. However, in this case, number of elements which is required for solving the complete radiator is extremely high due to the complex and repeating geometrical features of the radiator (more specifically the complex geometry of the fins). Such a large mesh cannot be handled efficiently even with today's computer technology. In this study, an alternative methodology is developed to use CFD as a design tool for the design of a fin-tube radiator. This methodology is based on the porous medium approach is developed. The number of elements in the computational

mesh has been decreased dramatically by modeling fin structures as a porous medium which makes CFD modeling a feasible tool to predict the thermal performance of a radiator.

In literature, porous modeling is governed by three models. The simplest model is the Darcy's model which is suggested by Henry Darcy (1856) during his investigations on hydrology of the water supplies of Dijon [2]. Darcy equation is expressed as,

$$\frac{\Delta p}{l} = -\frac{\mu}{\alpha} V \tag{1.1}$$

where, Δp is the pressure drop, l is the pipe length, V is the average velocity, μ is the dynamic viscosity and α is the permeability. Permeability depends on the fluid properties and the geometrical properties of the medium. Velocity in the Darcy's equation is linear; therefore, Darcy equation is used when the flow is laminar. As the velocity increases, non-linearity in velocity becomes prominent due to drag caused by solid obstacles. At this point, there are two extended models are proposed in the literature namely Forcheimer and Forcheimer-Brinkman model [2]. For moderate Reynolds numbers, including non-linearity effects is defined as Forcheimer's equation:

$$\frac{\Delta p}{l} = -\left(\frac{\mu}{\alpha} V + \frac{C_F}{\sqrt{\alpha}} \frac{1}{2} \rho V^2\right) \tag{1.2}$$

where C_F is the dimensionless form-drag constant and ρ is the density of the fluid. The first term denotes the viscous characteristics of porous flow and the second term denotes the inertial characteristics [2]. Last model is denoted as Forcheimer-Brinkman model. This model includes additional Laplacian term in addition to Forcheimer`s equation. Forcheimer-Brinkman model is expressed as [2],

$$\frac{\Delta p}{l} = -\left(\frac{\mu}{\alpha} V + \frac{C_F}{\sqrt{\alpha}} \frac{1}{2} \rho V^2 - \tilde{\mu} \nabla^2 V\right) \tag{1.3}$$

where $\tilde{\mu}$ is the effective viscosity. In general, added Laplacian term resolves effects of the flow characteristics in a thin boundary layer at the near wall regions. However, this effect is negligible in most practical cases; therefore, Forcheimer model is used generally [2].

Velocity definition in porous modeling is specified by using two different descriptions: superficial formulation and physical velocity formulation. Superficial velocity formulation doesn't take the porosity into account during the evaluation of the continuity, momentum and energy equations. On the other hand, physical velocity formulation includes porosity during the calculation of transport equations [3]. The continuity and momentum transport equation for a porous domain can be written as:

$$\frac{\partial}{\partial t}(\gamma\rho) + \nabla.(\gamma\rho\vec{v}) = 0 \tag{1.4}$$

$$\frac{\partial}{\partial t}(\gamma\rho\vec{v}) + \nabla.(\gamma\rho\vec{v}\vec{v}) = -\gamma\nabla p + \nabla.(\gamma\vec{\tau}) + \gamma\overrightarrow{B_f} - \left(\frac{\gamma^2\mu}{\alpha}\vec{v} + \gamma^3\frac{C_2}{2}\rho|\vec{v}|\vec{v}\right) \tag{1.5}$$

where γ is porosity, α is permeability of porous domain, C_2 is the inertial coefficient for porous domain and $\overrightarrow{B_f}$ is the body force term [3].

Besides flow modeling, heat transfer modeling for porous flow is described by using two models which are (i) equilibrium model and (ii) non-equilibrium model. Equilibrium model is used when the porous medium and fluid phase are in thermal equilibrium. However, in most cases fluid phase and porous medium are not in thermal equilibrium. For such cases, non-equilibrium thermal model is more realistic. The conservation equations of energy for fluid and solid are [3]:

$$\begin{aligned}\frac{\partial}{\partial t}\left(\gamma\rho_f E_f\right) + \nabla.\left(\vec{v}\left(\rho_f E_f + p\right)\right) \\ = \nabla.\left[\gamma k_f\nabla T_f - \left(\sum_i h_i J_i\right) + (\bar{\bar{\tau}}\vec{v})\right] + S_f^h + h_{fs}A_{fs}\left(T_s - T_f\right)\end{aligned} \tag{1.6}$$

$$\frac{\partial}{\partial t}\left((1-\gamma)\rho_s E_s\right) = \nabla.\left((1-\gamma)k_s \nabla T_s\right) + s_s^h + h_{fs}A_{fs}\left(T_f - T_s\right) \quad (1.7)$$

where E_f is total fluid energy, E_s is total solid medium energy, γ is the porosity, k_f is the fluid phase thermal conductivity, k_s is solid thermal conductivity, h_{fs} is heat transfer coefficient for the fluid/ solid interface and A_{fs} is interfacial area density that is the ratio of the area of the fluid/solid interface and the volume of the porous zone [3]. In the literature, non-equilibrium model is defined as a two equation energy model which can be utilized when the porous medium and fluid flow are not in thermal equilibrium.

1.1 Literature Review

In literature, porous medium studies are generally gathered in the area of fluidized beds, reactors and heat sinks. Modeling and analyzing heat exchangers with porous medium are quite rare. Presented studies related to porous medium approach and heat exchangers can be classified into three main groups. In the first group, porous modeling is utilized for the analysis of heat sinks [4-8]. For heat sink studies, generally volume-averaging method was used for porous modeling. Studies include analysis of micro heat sinks and macro heat sinks. In these works, generally analytical techniques were implemented and validated with the experiments, and volume-averaged modeling has been successfully implemented to determine the necessary flow and heat transfer characteristics [4-7]. In the second group, the studies comprising computational modeling, are focused on some specific sub-components of the heat exchangers [10-23]. These studies includes the analysis of flow over the fin structures [10-15, 18, 19, 22, 23], analysis of flow through a fan located at the inlet of the radiator [19], analysis of maldistribution in header parts [13, 20, 21] of a radiator. In many of these studies [10, 11, 15, 20, 21], the computational model is validated with respect to the experimental results, and it is observed that computational modeling is prosperous tool for the determination of flow and heat transfer characteristics for such components and flow domains. In the third group, studies focused on the analysis of full-sized heat exchangers

implementing different computing methodologies [21-34]. In these studies, various types of heat exchangers such as Z type cross-flow heat exchanger [22], matrix type of heat exchanger [23], lotus type heat exchanger [25], plate-fin heat exchanger [27] and many other types [21, 24, 26, 28-33] are analyzed. In many studies, porous medium approach was utilized in order to model fin structures. Outcomes of these studies illustrate the heat transfer and fluid flow characteristics of heat exchangers. Computational results have been validated with the results from the literature [26, 27] and the experimental results [22-31]. Additionally, some studies include only experimental analysis [32, 33].

Modeling of the heat sinks includes some fin structure modeling. However, the fin structures used are in the form of perforated plates and they are not similar to the fin structures used in the radiators. Do et al. [4] conducted an analytical study for the thermal optimization of internally axial finned tube. Problem consists of two domains, which are the porous region where fins are located, and the fluid region that is the remaining void flow domain. Porous domain was modeled with Brinkman-extended Darcy equation, and two-equation heat transfer model was used for the heat transfer modeling. The friction factor, velocity and temperature profiles at certain locations were compared with the numerical and experimental results from the literature for the validation, and agreement was achieved. Based on the developed analytical model, an optimization was also performed for an internally finned tube. Kim et al. [5] analytically modeled micro-channel heat sinks as a porous medium. Brinkman-extended Darcy and two-equation heat transfer model were used for the fluid flow and heat transfer analysis, respectively. The analytical solutions were compared with the numerical solutions. Analytically obtained volume averaged velocity and temperature distributions were well matched with the numerical solutions. They discussed the effects of aspect ratio and effective thermal conductivity ratio on the thermal performance of a micro-channel heat sink. Kim and Kim [6] analyzed a straight finned heat sink using a compact modeling method based on volume-averaging technique analytically. Momentum and energy equations were obtained by using local volume-averaging method. Experimental analysis was utilized, and temperature and pressure drop results were compared. It was observed

that the analytical and experimental pressure and temperature drop results were well matched with each other. Jeng and Tzeng [7] were determined the porous medium characterization coefficients to be used in Forcheimer model for pin-fin heat sinks by using a semi-empirical method. They obtained the experimental data by placing the porous structure in a wind tunnel with variable test section height. Jeng et al. [8] proposed a technique using fin theory and thermal network concept to estimate the heat transfer from a porous heat sink. They used Forcheimer-Brinkman equation to model fluid flow through porous medium and two-equation model was used for the thermal analysis. The viscous and inertial coefficients and the heat transfer coefficient between the solid and fluid phases were taken from the studies in the literature. They concluded that thermal network approach by using fin theory is more practical than other available numerical techniques, and can accurately predict the convection heat transfer in metal foam and sintered porous channels.

Considering the analysis of heat exchangers, there are techniques available such as log mean temperature difference (LMTD) and epsilon-NTU. However, these techniques require some predefined parameters such as overall heat transfer coefficients and/or NTU relations for a given heat exchanger. There are no general expressions valid for any heat exchanger Therefore, these parameters needs to be predicted either from an experimental data and/or analytical expressions [9]. On the hand, a heat exchanger can be analyzed by utilizing a CFD analysis. However, CFD analysis of a full-size heat exchanger is not feasible due to complex nature of the heat exchangers especially the fin structures. Therefore, CFD analysis of heat exchangers with complex fin structures were conducted on specific sub-components and separate domains of heat exchangers such as unit cell fin, radiator fan and air-side or fluid-side flow and heat transfer characteristics. Kulasekharan et al. [10] investigated the improvements of fin-tube type heat exchangers performance by focusing on fin performance improvement. In their study, flow and heat transfer characteristics for louvered fin were investigated by using both experimental and numerical methods. Physical unit cell louvered fin model with tubes was analyzed by using commercial CFD code FLUENT® 13.0. Turbulence modeling determination was specified from the literature and selected as k-ω turbulence model. Numerical

solutions were validated by the experimental data that were taken from literature. Pressure drop across the fin, outlet water and air temperatures and heat transfer rate parameters were compared. According to the results coherence was obtained in reasonable limits. Wen et al. [11] has conducted an experimental study on a plate fin, wavy fin and compounded fin in order to obtain heat transfer and pressure drop characteristics of each fin. Series of experiments were utilized for three types with respect to varying Reynolds numbers. Pressure drop across the fins, friction factors and heat transfer coefficients were obtained through experiments. Results of the experiments show that compounded fin has highest heat transfer coefficient when compared with others; however, compounded fin also maintains the highest pressure drop with respect to others. Similar to Wen et. al. [11], Yan and Sheen [12] investigated pressure drop and heat transfer characteristics of plate, wavy and louvered fins experimentally. Friction factors, Colburn factors and heat transfer coefficients were investigated with respect to varying Reynolds numbers. Louvered fin has the highest heat transfer coefficient when compared with the other types; however it has higher pressure drop when compared to others. Additionally, by using obtained friction and Colburn factors from fins, thermal performance of complete heat exchangers was calculated by using ε-NTU method. Ismail et al. [13] studied thermo-hydraulic design of a compact heat exchanger. Computationally, Colburn factor and Fanning friction factors were obtained with respect to varying Reynolds numbers for the wavy fin configuration. Additionally, flow maldistribution in the headers was analyzed computationally on three different compact plate-fin heat exchanger configurations. The effects of nozzle orientation on thermal performance in headers were investigated through header flow distribution simulations. Remarks of the results indicate that uniform flow distribution in the header increases thermal performance of the heat exchanger which depends on the nozzle orientation at the headers. Numerical simulations were conducted by using commercial code FLUENT®. Colburn and Fanning friction factors of wavy fin results were validated with analytical and experimental results obtained from the literature. Dejong et al. [14] investigated the fluid flow and heat transfer characteristics of offset strip-fin arrangement. They utilized both numerical and experimental analysis. Colburn factor, friction factor and Nusselt number for offset strip-fin arrangement were

obtained from the experimental and numerical simulations and results were compared with the ones in the literature. Coherence was obtained between results, and it was observed that for Reynolds numbers higher than 1300, the development of boundary layer, flow separation and vortex shedding characteristics varies with respect to 3-dimensional effects. You and Chang [15] utilized experimentation in order to obtain porous medium flow coefficients for the uniformly distributed square pin fins. Pressure drop values were collected with respect to varying input velocities. Brinkman-Forcheimer relation was used in order to determine the permeability and inertial coefficient of square pin fins. Determined permeability and inertial coefficients were compared with the results in the literature and coherence was obtained. Effects of porosity variation was also observed and it is seen that permeability increases rapidly as the porosity increases; however, inertial coefficient doesn`t change significantly as the porosity increases. Zukauskas and Ulinskas [16] conducted experimentation in order to investigate the pressure drop and heat transfer characteristics for staggered tube banks. Analyses were conducted with respect to variable Reynolds numbers, Prandlt numbers and varying transverse and longitudinal pitch sizes between tubes. Efficiency factor of tube banks obtained from experimentation was compared with the results in the literature, and coherence was obtained. Optimization process was performed and optimum tube bank design was obtained. Varol et al. [17] conducted a numerical study by using the finite difference method. Model is described as a two-dimensional solid thin fin attached to a porous right triangular enclosure. Porous domain is modeled with Darcy's equation. Lower wall of the triangular enclosure is heated, left wall is insulated and right wall is cooled at constant temperature. By changing the location of the fin, streamlines and variation of local Nusselt number along the hot wall were obtained. According to the results, it is concluded that the fin is considered as a passive control parameter for heat transfer and fluid flow. Yang et al. [18] numerically analyzed forced convection in three-dimensional porous pin finned channels. Analyses were conducted with respect to variable fin geometries with variable sizes. They used Forcheimer-Brinkman model for flow characterization and two-equation energy model for the heat transfer characteristics of porous domain. Inertial, viscous and heat transfer coefficients were calculated from the derived analytical formulations available in the

literature. Results are investigated using pressure drop and heat flux characteristics with respect to porous fin and solid fin configurations. It was concluded that by using optimized porous pin fin, pressure drop decreases and heat transfer from porous pin fin increases. Jain and Deshpande [19] were studied air-flow characteristics for radiator fan. In their study, they investigated the flow characteristics of fan and how it affects the inlet of the air-side of radiators. Commercial model of the axial fan was used in their analysis. Pressure drop and velocity distribution characteristics were obtained from numerical simulations and pressure drop values were validated against experimental data. Header flow characteristics of plate fin heat exchangers were investigated by Zangh and Li [20]. They focused on flow maldistribution in header part of the heat exchanger. It is stated that the header flow distribution essentially affects the heat transfer characteristics of the heat exchanger due to the uniformity of flow distributions. Numerical analysis was performed on a conventional header configuration by using commercial CFD code FLUENT®. Average flow velocities at the inlet of the channels obtained from numerical analysis were compared and validated with the experimental data. Optimization was performed on header by modifying geometrical parameters of the header using numerical analysis. Similar to Zangh and Li [20], Wasevar et al. [21] analyzed the header flow distribution characteristics of plate-fin heat exchangers. Numerical analysis was conducted by using commercial software FLUENT®. They concluded that the uniform distribution across the tubes is almost impossible due to inlet header configuration. However, optimized location of pipe and geometry can produce the optimized uniformity in the tubes. With optimized header design, heat exchanger efficiency is increased. In their study, they used computational model for the analysis. They first analyzed the conventional header of heat exchanger and modifications were made on the design due to the flow distribution. Conclusions of their study emphasize the fact that modification increases the uniformity across the tubes. Numerical analysis was utilized by Baliga and Azrak [22] on triangular plate fin arrangement. They described the problem as a triangular duct and analyzed heat transfer characteristics of the fin. They used finite volume method for numerical discretization. According to their study heat transfer characteristics were obtained numerically for triangular plate fins. Similar to Baliga and Azrak [22], Zangh [23], focused on the interaction of heat

transfer characteristics with the varying apex angles of triangle plate fins. In their study, fin conductance parameters were obtained with respect to the varying apex angles. Study leads a way to, estimate the thermal performance of plate fin compact heat exchangers by using obtained conductance parameters from the numerical analysis. It was concluded that the variation of apex angles changes the heat transfer characteristics essentially.

So far, studies in literature on fin structures and component based analysis are described. In literature, there also researches which have been carried on varying type of heat exchangers with different methods. Oilet et al. [24] investigated the influence of input parameters (inlet mass flows, temperatures, etc.) on thermal and flow characteristics of vehicle radiators numerically. The numerical methodology based on discretization of whole radiator domain into macro control volumes (not small control volumes used in CFD analysis) was developed. Outcomes of their study illustrates the variation fluid flow and heat transfer characteristics of heat exchanger with respect to the varying input parameters such as; coolant inlet mass flow rate, air velocity, coolant inlet temperature and air inlet temperature, and some handy design tips on the design of vehicle radiators. The validation and verification of the numerical results were performed by using experimental data. Zangh [25] investigated the flow distribution characteristics and thermal performance of air-to-air cross flow heat exchangers. The arrangement of the heat exchanger is Z-type, which maintains a non-uniform flow on the core surface. Due to this non-uniformity in the flow thermal performance is affected. Heat exchanger was modeled as a porous medium. Analysis of flow distribution of the heat exchanger was performed by using FLUENT®. Obtained flow distribution data were used for the determination of heat exchanger effectiveness and thermal performance deterioration by implemented ε-NTU based finite difference scheme. Porous modeling was performed by using the Darcy's equation. Permeability of the medium was obtained from an analytical correlation. Numerical results of velocity non-uniformity and thermal deterioration factors were validated with experimentation. Results show that modeling heat exchanger, as a porous media is acceptable and sufficient to observe non-uniformity effects on thermal deterioration. Hayes et al. [26] studied both heat

transfer and fluid flow characteristics on matrix heat exchanger. Analysis was conducted by using developed two-dimensional numerical model and FLUENT®. Friction factor, temperature distribution across the domain and local heat transfer coefficients obtained from the computational analysis were validated with experimental results. Porous modeling of two-dimensional numerical model was obtained from Brinkman-Forcheimer relation; on the other hand, for FLUENT® analysis Forcheimer relation was used. Inertial and viscous coefficients were obtained from the experimental pressure drop data. According to the results two-dimensional model was modified and correlated with respect to the FLUENT® and experimental results. Mao et al. [27] performed a comprehensive study on heavy-duty truck radiators. Their work is based on thermal and structural analysis of a radiator. FLUENT® commercial code was used for the thermal analysis. For thermal analysis, either air-side where fins are located or fluid-side where tubes are located with turbulator fins, were modeled as a porous medium which is defined as dual porous zone method. Forcheimer relation is used for porous modeling and viscous and inertial coefficients were determined with respect to the experimental pressure drop data across the fin and turbulator. One equation energy model is used with averaged equivalent thermal conductivity input parameter. Obtained local heat transfer coefficients and pressure distribution from the thermal analysis were used as a boundary condition for finite element structural analysis. From the structural analysis, thermal stresses and strains were obtained. Obtained maximum stress/strain in structural analysis was validated with the experimental results and concurrency was obtained. Ogushi et al. [28] studied heat transfer characteristics and capacities of lotus-type of heat sinks. They examined the thermal conductivity and heat capacity of lotus-type copper straight fined heat sink model. Study was examined in three parts. At first, effective thermal conductivity of lotus copper was investigated through experimentation with respect to the pore effect on heat flow. Then by using the obtained effective thermal conductivity, the lotus copper straight fin was analyzed numerically for obtaining the heat transfer capacity of heat the sink. Finally, the determined heat capacities were compared with the experimental data. According to the results, it is seen that lotus-type copper heat sinks heat transfer capacities are four times greater than conventional groove finned heat sinks.

Carluccio et al. [29] examined the thermo-fluid analysis of compact cross flow heat exchanger that is used for cooling oil circulating in hydraulic circuits. They analyzed small-scaled section of heat exchanger then passed on to the large scaled original model. Large-scale model was analyzed by using porous medium approach with Forcheimer relation as a porous model. Inertial and viscous coefficients were obtained from the small scale analysis. For fins, Colburn factor, Fanning friction factor and heat transfer coefficient were obtained from the small-scaled numerical simulations and compared with the results obtained from the literature. Additionally, oil side pressure drop and local heat flux were obtained from small-scale model. Overall heat transfer coefficients and global pressure drop characteristics were obtained numerically from large-scale model. Wang et al. [30] studied the plate-fin heat exchangers with respect to hydro-dynamical point of view. They used porous medium approach to obtain flow characteristics for full sized plate-fin heat exchanger. In their study, unit cell fin simulations were conducted, in order to obtain porous medium flow coefficients. Forcheimer relation was used for porous medium flow characterization. Friction factor results were validated with the experimental results that were obtained from literature. Porous coefficients were implemented into full-sized model and simulated. Pressure drop across the heat exchanger with respect to varying Reynolds numbers were obtained and experimentally validated. Pavel et al. [31] investigated gas heat exchangers that are filled with metallic materials both experimentally and numerically. Gas heat exchangers are another heat exchanger type that is described as a pipe and metallic porous materials filled inside. Inside pipe is modeled as a porous domain and pipe is subjected to the constant heat flux. Forcheimer relation was used for porous modeling and inertial and viscous coefficients were determined from experimental pressure drop data. Numerical model was based on finite difference method. Results of the study were investigated under varying porosity parameters and Reynolds numbers. Pressure drop, heat transfer rate and effective thermal conductivity parameters are compared between numerical and experimental analysis and coherence was obtained. Conclusions of their study exposes the fact that higher porosity values leads higher heat transfer rates, however, it also increase pressure drop either. Yu et al. [32] studied air-water heat exchangers with carbon-foam coated fins. Parametric study was performed and

experimentation was utilized. Results were investigated for varying porosity and pore diameter of carbon-foam. Forcheimer relation was used for porous modeling of carbon foam and inertial and viscous coefficients were obtained from analytically derived formulations. According to the results it is seen that carbon-foam exposed aluminum fin and tube type of radiator has 15 % increase in thermal performance with respect to non-carbon foamed radiator. Aydar and Ekmekçi [33] conducted CFD analysis on panel type radiators by using commercial code Star-CCM+. They focused on thermal efficiency of a radiator. First air-side convective heat transfer coefficient is analyzed and inputted into radiator analysis as a boundary condition at outer wall boundaries. Thermal efficiency results obtained from numerical analysis were compared with the catalog values of analyzed commercial radiator and coherence was obtained. Gullapallı and Sundén [34] conducted a study on corrugated channels of compact brazed-plate heat exchangers. Corrugated flow passages of heat exchanger are analyzed for both thermal and hydro-dynamical aspects by using ANSYS CFX commercial code. By modifying sizing parameters such as; chevron angle and corrugation pitch, variation of thermal and hydro-dynamical characteristics were observed. Additionally thermal performance improvement was determined with respect to analyzed characteristics. Nusselt number and pressure drop results obtained from the numerical analysis were validated with respect to experimentation and 20-30% contrast is obtained on heat transfer and 10-35% contrast is obtained from pressure drop characteristics. Taler [35] investigated heat transfer coefficients on both fluid sides of cross-flow heat exchangers experimentally. Correlation coefficients are obtained with respect to experimentation based on weighted least squares method and analytical model is generated which estimates the outlet temperatures of air and liquid sides. By using experimental data, outlet temperature on the fluid-side and air-side were obtained from developed analytical model. Apart from macro sized heat exchangers Yang et al. [36] conducted an experimental study on micro-combustor radiators. Micro-combustor radiators are used in micro-thermo photovoltaic systems. In gas-side of radiators, SiC foam was inserted into a micro modular combustor and experiments were performed with respect to filled and non-filled foam configurations. According to the results, foam insertion increases the wall temperature around 90 to 120 K and this increase leads the way through increase in

radiation energy that is proportional with electricity generation. Another micro system heat exchanger analysis was carried out by Jiang et al. [37]. They studied hydrodynamic and thermal characteristics of micro heat exchangers by using experimentation. Experiments were conducted on two types of micro heat exchangers which are the micro-channel heat exchanger (MCHE) and micro porous heat exchanger (MPHE). MCHE model is defined as micro-scale finned cross-flow heat exchangers; on the other hand, in MPHE model porous material is inserted into channels instead of fins. Results indicate that the pressure drop across MCHE is much lower than the MPHE; on the other hand MPHE has higher heat transfer performance with respect to the MCHE.

As discussed so far, there have been many studies considering the determination of flow and heat transfer characteristics for either a single component or for a complete heat exchanger. In many studies, fin structures are modeled with porous medium approach due to their complex and periodic shape characteristics. It has been proven that porous modeling is an efficient tool to model the flow and heat transfer characteristics of the fin structures. Considering the 3-D modeling of full-sized compact heat exchangers especially the vehicle radiators, there are very few studies recently (after 2004) available in the literature [24,25,27,29]. There is only one study considering the CFD modeling of a full-sized vehicle radiator [27]. In their work one-equation model for the energy equation is utilized which is not an appropriate model especially when there is an appreciable temperature difference between the fin structure and the fluid. In this thesis study, a 3-D CFD modeling of a full-sized vehicle radiator is performed by using porous modeling for the modeling of fluid flow and heat transfer on the finned structures. Forcheimer model and two-equation model for the energy equation are implemented. Commercial CFD code, FLUENT® is used in this study. The cooling capacity of a tractor radiator is computed with the proposed computational model and compared with the catalog data of the same radiator.

1.2 Outline of the Study

CFD modeling proposed in this thesis is composed of three phases. The pre-processing phase involves fin-side (air-side) porous medium modeling, water-side modeling, meshing and setting up the necessary parameters. In the solution phase, the solution method is selected, relaxation factors are tuned up and solution is performed. Finally, in the post-processing phase, the results are processed. For CFD analysis, commercial software ANSYS 14.5 workbench is used with FLUENT® 14.5.

The water domain of the radiator was modeled as a regular fluid domain while the air domain was modeled as a porous medium due to the complex and repeating geometry of fins. Implementation of fins into air domain is maintained by using porous media on the air side. In order to obtain the necessary input parameters and coefficients for porous medium, separate simulations were performed on a unit cell with straight fin and wavy fin structures. Procured porous medium parameters are implemented into full-sized radiator model and fluid flow and thermal analysis is utilized. Outcome of the study presents the prediction of a thermal performance of an industrial vehicle radiator.

In Chapter 2, porous modeling of unit cell straight fin and wavy fin is covered. Extraction of porous medium flow and heat transfer parameters are discussed in this chapter. In Chapter 3, the analysis of full-sized 2x10-tube reduced radiator model and 4x39-tube real life application model are presented under both hydro-dynamical and thermal point of views. In Chapter 4, the conclusion of the study is presented.

CHAPTER 2

POROUS MODELING

In this chapter, porous modeling of the fins of the radiator is explained extensively. Porous modeling is applied on the air-side of the radiator to replace the physical fin with a porous medium. . In order to start with basics, first of all a straight fin configuration is analyzed then wavy fin that is used in real life radiator applications is analyzed. Chapter continues in the order of; determination of porous medium coefficients, 38 mm straight fin porous modeling involving analytical analysis, mesh independency, turbulence model selection, porous medium property extraction and comparison of results between physical and porous fins and 84 mm wavy fin porous modeling involving mesh independency, porous medium property extraction and comparison of results between physical and porous fins.

2.1 Determination of Porous Medium Coefficients

Mathematical modeling of porous domain is governed by the continuity, momentum and energy equations that are presented in equations (1.4) through (1.7). Additionally, Forcheimer relation presented in equation (1.2) is used for porous modeling. The extraction of the porous medium coefficients is obtained by using the unit cell fin models. The coefficients are extracted from the velocity versus pressure plot. Procedure is performed by the following steps [3]:

(a) Simulation of the unit cell fin model is performed by implementing varying input velocities and then the calculated pressure drops across the fin are tabulated.

(b) A second order curve is fitted to the collected pressure versus velocity data to obtain the Forcheimer relation as,

$$\frac{\Delta P}{l} = a\,V + b\,V^2 \tag{2.1}$$

where *a* and *b* are the coefficients characterizing the flow.

(c) From the obtained coefficients, the inertial coefficient and viscous coefficient can be obtained as:

$$Inertial\ coefficient\ = \frac{2\ b}{\rho\ l} \tag{2.2}$$

$$Viscous\ coefficient\ = \frac{a}{l\,\mu} \tag{2.3}$$

After obtaining the flow based porous medium coefficients, the next step is to obtain the heat transfer input parameters. The necessary input parameters are the average heat transfer coefficient (*HTC*) and interfacial area density (IAD) for the non-equilibrium thermal model that is described in equations (1.6) and (1.7). Average heat transfer coefficient is obtained from FLUENT post-processing which can be calculated by using following relation [3]:

$$HTC = \frac{Q}{T_w - T_{ref}} \tag{2.4}$$

The reference temperature in the above equation is taken as the average temperature between the inlet and outlet of the fin. Interfacial area density can be found from the CAD model which can be defined as the ratio of the area of the fluid/solid interface to the volume of the porous zone [2].

2.2 Straight Fin Porous Modeling

The purpose of unit cell straight fin simulations is to obtain the flow and heat transfer characteristic parameters of the porous medium. Unit cell straight fin simulations are analyzed in two parts which are the physical fin simulations and porous medium fin simulations. In physical fin model simulations, the exact geometry of the fin is placed in the air stream, while porous domain is located in the stream for porous medium fin model simulations. These simulations are carried out to compare the pressure and temperature drop characteristics across the fin for physical and porous fin simulations.

2.2.1 Analytical Analysis

To determine the turbulence model to be used in the mathematical model, the pressure drop across the fin is evaluated analytically by considering the blockage due to the development of the viscous boundary layer along the walls of the fin. The geometry of the 38 mm straight fin is shown in Figure 2.1. The flow outside the boundary layer is assumed to be inviscid and the pressure drop due to the reduction in the ideal flow area is calculated to be approximately 197.9 Pa by using Bernoulli equation. Following procedure presents the analytical formulation [38]:

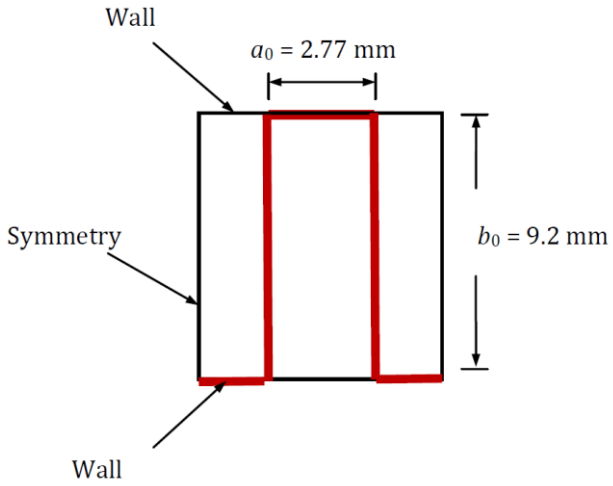

Figure 2.1: Geometry of 38 mm Straight Fin (Front View)

The Reynolds number at the end of the fin is:

$$\mathrm{Re}_L = \frac{\rho UL}{\mu} = \frac{(1.2\ \mathrm{kg/m^3})(20\ \mathrm{m/s})(0.084\ \mathrm{m})}{0.000018\ \mathrm{Pa.s}} = 1.12\times10^6 \tag{2.5}$$

Therefore, the flow is laminar. If the fin thickness is taken into consideration;

$$a = a_0 - t \tag{2.6}$$

$$b = b_0 - t \tag{2.7}$$

are obtained. At the inlet, the flow area can be obtained as;

$$A = ab \tag{2.8}$$

At a distance of *x* distance from the inlet of the fin, the boundary layer displacement thickness can be calculated from;

$$\delta_d = 1.721\sqrt{\frac{\mu\ x}{\rho\ U}} \tag{2.9}$$

In this case fin width and height are;

$$a' = a - 2\delta_d \tag{2.10}$$

$$b' = b - 2\delta_d \tag{2.11}$$

As a result, flow area at a distance of *x* from the inlet becomes;

$$A' = a'b \tag{2.12}$$

By using continuity equation, flow velocity is calculated as;

$$V' = \frac{AV}{A'} \tag{2.13}$$

Additionally, pressure drop is calculated as;

$$\Delta p = \frac{1}{2}\,\rho\,(V'^2 - V^2) \tag{2.14}$$

Pressure drop along the fin is illustrated in Figure 2.2:

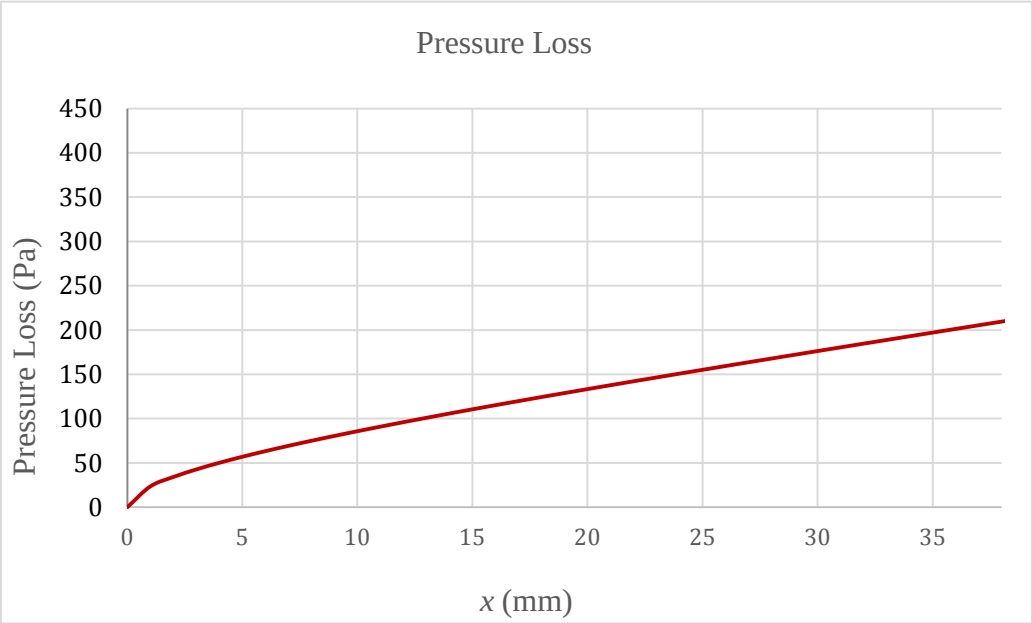

Figure 2.2: Pressure Drop Along the Fin

2.2.2 Physical Fin Simulations

Simulations are carried out in two steps. First, a unit cell of the straight fin (SF) model, referred to as Model-A (Figure 2.3-(a)), is analyzed in order to obtain porous media characteristics.

However, porous medium model doesn't recognize the expansion and contraction characteristics at the inlet and outlet of the fin. For this reason, Model-B, which is a unit cell of the straight fin with additional upstream and downstream domains as seen in Figure 2.3-(b), was analyzed. Porous jump boundary conditions are introduced to match the results of the Model-B of physical fin and porous medium model simulations.

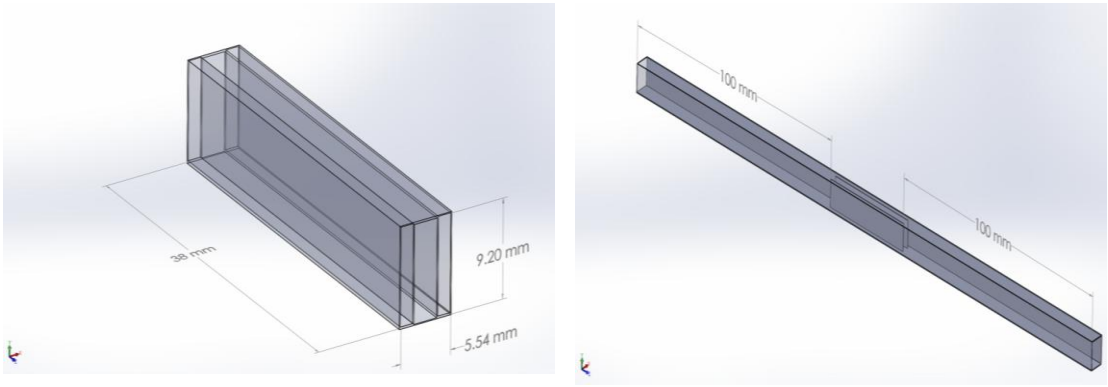

(a) **(b)**

Figure 2.3: **(a)** Model-A: SF Unit Cell Domain, **(b)** Model-B: SF Unit Cell with Additional Inlet and Exit Domains

For Model-A are set as: velocity inlet and pressure outlet boundary conditions are used for the inlet and exit of the straight fin. Wall boundary condition is assigned to the upper and lower walls, while periodic boundary condition is used for right and left sides. For Model-B, additionally symmetry boundary condition is assigned for upstream and downstream domains.

For both simulations, SIMPLE method is used with least square based cell approximation. Additionally; standard scheme for pressure and second order up-winding schemes for momentum, turbulent kinetic energy and turbulent dissipation rate are employed. Relaxation factors are set to their default values. For both simulations, a minimum convergence of $1x10^{-5}$ was obtained for all residuals.

2.2.2.1 Mesh Independency

Comprehensive mesh independency analysis is performed on Model-A. Model-B has the same geometry but it has additional upstream and downstream domains so that the selected boundary layer mesh and sizing parameters for Model-A is applied to Model-B. However tetrahedron elements are used due to the geometry of Model-B. Nine different hexa-type mesh configurations are simulated and the same boundary layer mesh is used for all configurations. Table 2.1 and Figure 2.4 illustrate the result of the mesh independency analysis.

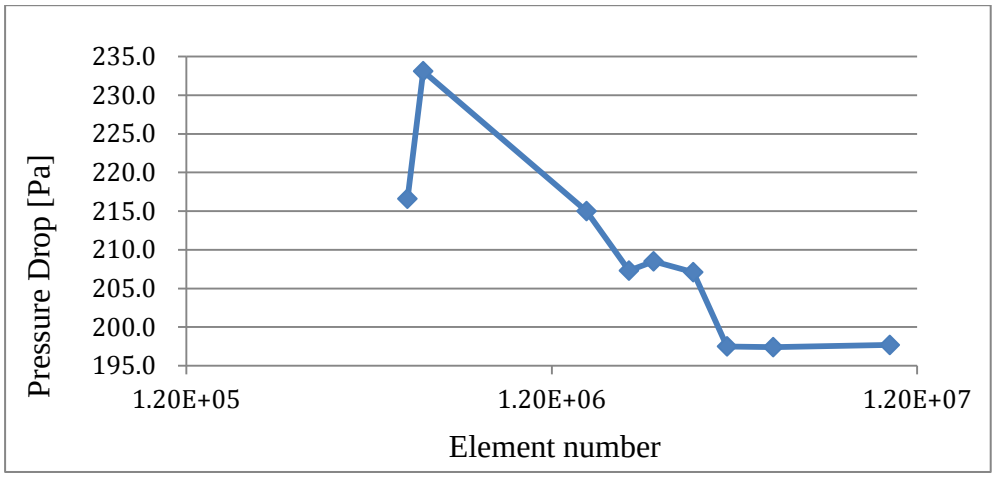

Figure 2.4: Mesh Independency Plot for Model-A

Table 2.1: Mesh Independency Analysis

	Element Number	Pressure Drop [Pa]	Skewness
Mesh 1	483,208	216.6	0.223
Mesh 2	533,781	233.1	0.237
Mesh 3	1,494,536	215.0	0.185
Mesh 4	1,952,752	207.3	0.192
Mesh 5	2,280,380	208.5	0.165
Mesh 6	2,928,470	207.1	0.190
Mesh 7	3,624,060	197.5	0.220
Mesh 8	4,847,280	197.4	0.019
Mesh 9	10,108,380	197.7	0.180

According to the results, seventh mesh configuration containing 3,624,060 elements is selected for the Model-A (Figure 2.5-(a)) simulations. For the same mesh parameters, Model-B is meshed and a mesh with 6,125,667 elements are generated (Figure 2.5-(b)).

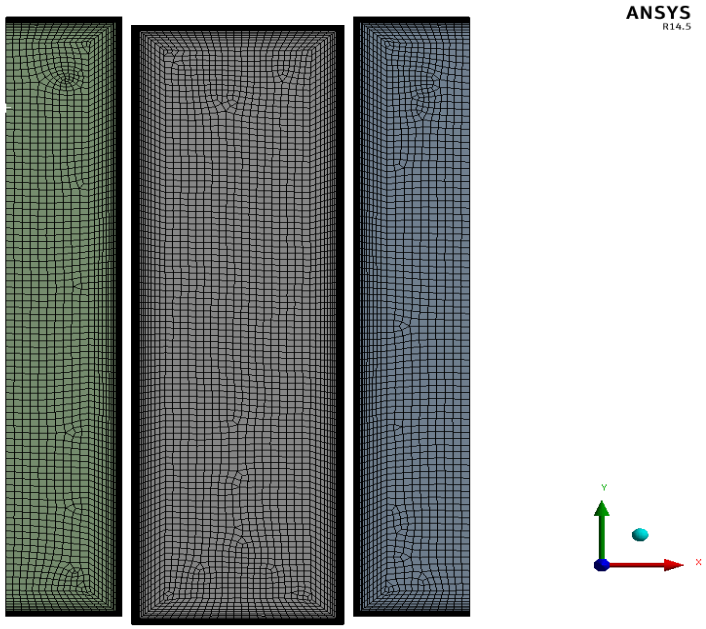

(a)

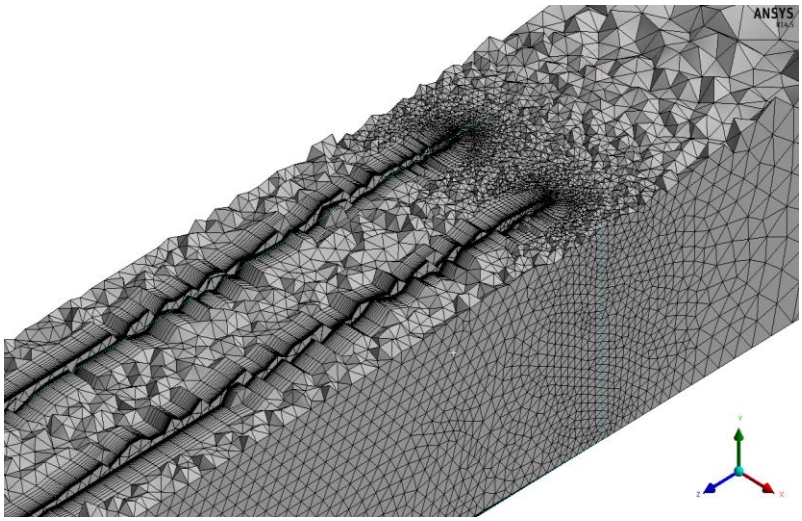

(b)

Figure 2.5: **(a)** SF Model-A mesh Configuration, **(b)** SF Model-B mesh Configuration

2.2.2.2 Turbulence Model

Based on comparison with analytical results, among the turbulence models that are compared, *k*-ε realizable turbulence model with standard wall functions produced the best approximation to this pressure drop. Table 2.2 presents the pressure drop values and Figure 2.6 illustrates the comparison of sectional averaged pressure drop for different turbulence models and the analytical solution:

Table 2.2: Pressure Drop for Different Turbulence Models

Turbulence Method	Pressure Drop [Pa]
k-omega standard	135.3
k-omega SST	132.1
k-epsilon Standard	235
k-epsilon RNG	229
k-epsilon Realizable	197.5
Analytical	197.9

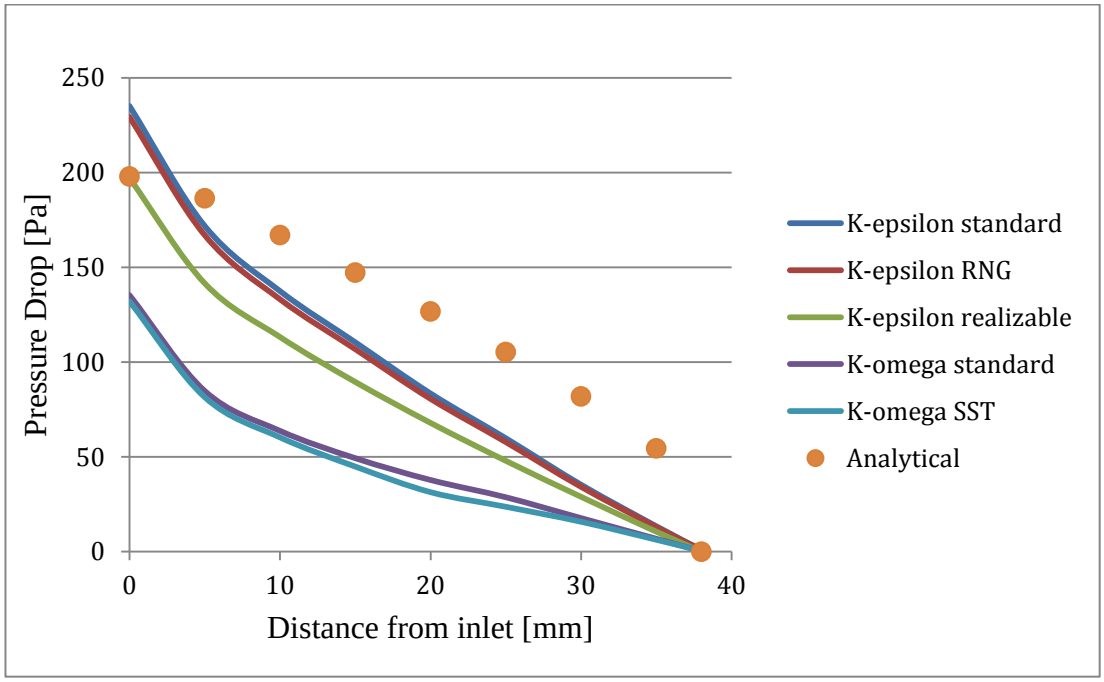

Figure 2.6: Turbulence Models Comparison with Analytical Solution

2.2.2.3 Extraction of Porous Model Parameters

Flow parameters are obtained by using Forcheimer relation. Model-A is simulated under different Reynolds numbers and Forcheimer curve is obtained. Table 2.3 contains the input parameters for the Model-A. In Figure 2.7, pressure is plotted against velocity and a second order curve is fitted to the simulation data. The corresponding inertial and viscous coefficients are determined to be 14.3 and 4.47×10^6, respectively.

Table 2.3: Input Parameters for Unit Cell Straight Fin Simulations

	DESCRIPTION	Unit
Domain length	38	mm
Element number	3,624,060	
Skewness (average)	0.22	
Turbulence modeling	k-ε-realizable	
Fin volume	108.07	mm^3
Total volume	1936.8	mm^3
Porosity	0.9442	
Hydraulic diameter	0.00241	m
Turbulence Intensity	0.053	
Turbulence length	0.000169	m
Solution method	SIMPLE	
Computation time	11	mins

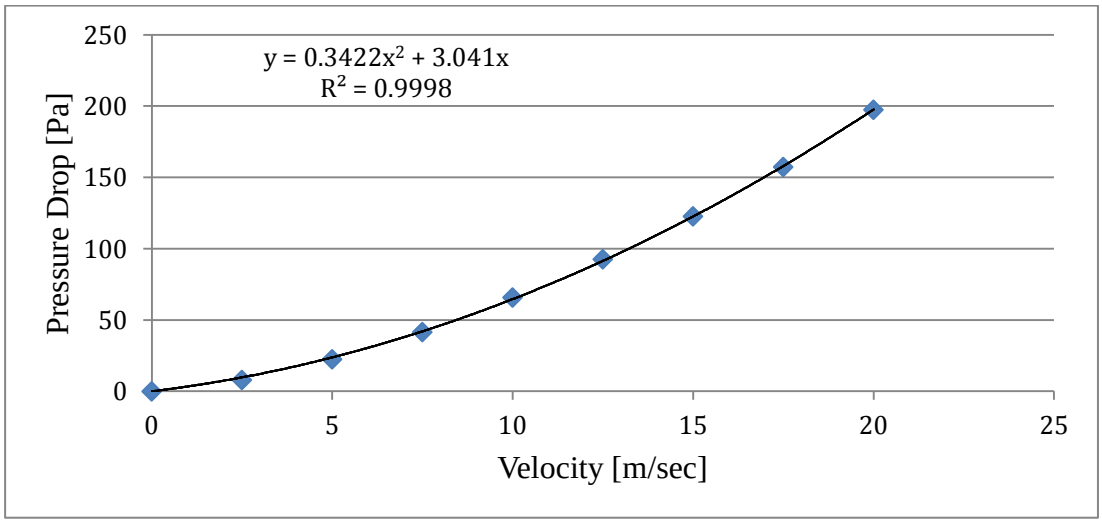

Figure 2.7: Unit Cell Physical SF Simulation Pressure versus Velocity Plot

Heat transfer parameters are obtained from Model-B simulation. For Model-B simulation input parameters are defined as; 7 m/s for the inlet velocity, 304.15 K for the inlet temperature and 359.65 K for the temperature of fin walls. Average surface heat transfer coefficient and tuned porous jump coefficients for the unit cell of a straight fin are presented in Tables 2.4 and 2.5, respectively.

Table 2.4: Heat Transfer Characteristics for a Unit Cell of a Straight Fin

Interfacial area [m^2]	Porous volume [m^3]	IAD [1/m]	HTC [W/m^2-K]	T_{ref} [K]
0.001567621	$1.93678x10^{-6}$	809	133	321

Table 2.5: Porous Jump Coefficients for a Unit Cell of a Straight Fin

	Face permeability [$1/m^2$]	Thickness [m]	Inertial coefficient [1/m]
Inlet	$4.47x10^{6}$	0.1	1.54
Outlet	$4.47x10^{6}$	0.1	-3.6

2.2.3 Straight Fin Simulations with Porous Modeling

Similar to the physical fin simulations, porous fin simulations are conducted by using the same process. However, in this case, simulations are conducted only under unit cell of the porous straight fin domain with additional upstream and downstream domains attached as seen in Figure 2.8-(a). Afterwards, the comparison is made between this model and Model-B of physical fin simulations.

For porous fin model, hexa-sweep meshing is used. The mesh of the porous model (Figure 2.8-(b)) consists of 2,574 elements with a skewness of $1.305x10^{-10}$. The most significant advantage of the porous medium mesh is that it doesn't require any boundary layer mesh. Therefore, this model requires considerably a lower mesh size and has a better convergence characteristic.

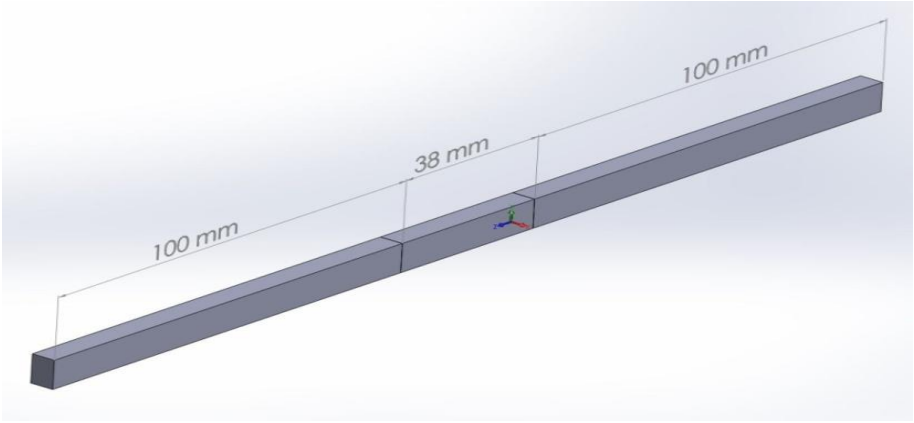

(a)

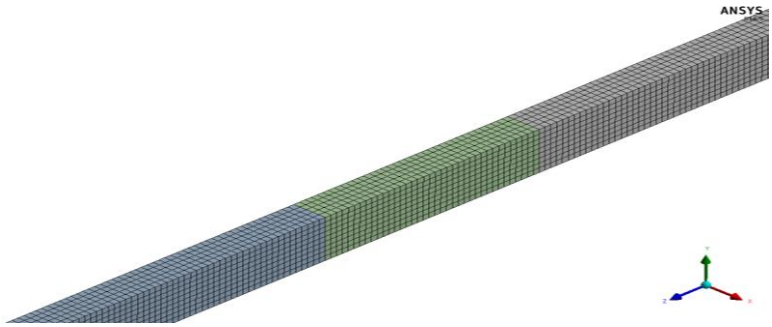

(b)

Figure 2.8: **(a)** Unit Cell Porous SF with Additional Inlet and Exit Domains **(b)** Mesh Configuration

After completing meshing process, boundary conditions are assigned. Besides the physical fin boundary condition configuration, additional porous jump boundary conditions are assigned to the inlet and outlet of the porous domain as porous medium boundary conditions. All FLUENT solver settings are taken to be the same as the physical fin simulations.

2.2.4 Comparison and Discussion

After porous medium flow coefficients, porous jump coefficients and heat transfer parameters are obtained from the simulation of a unit cell of a straight physical fin, porous medium simulations are analyzed with the same input parameters and comparison is made. Figure 2.9 compares the sectionally averaged pressure drop for

the physical fin and porous medium. Figure 2.10 shows the same comparison for the sectionally mass flow averaged temperature drop.

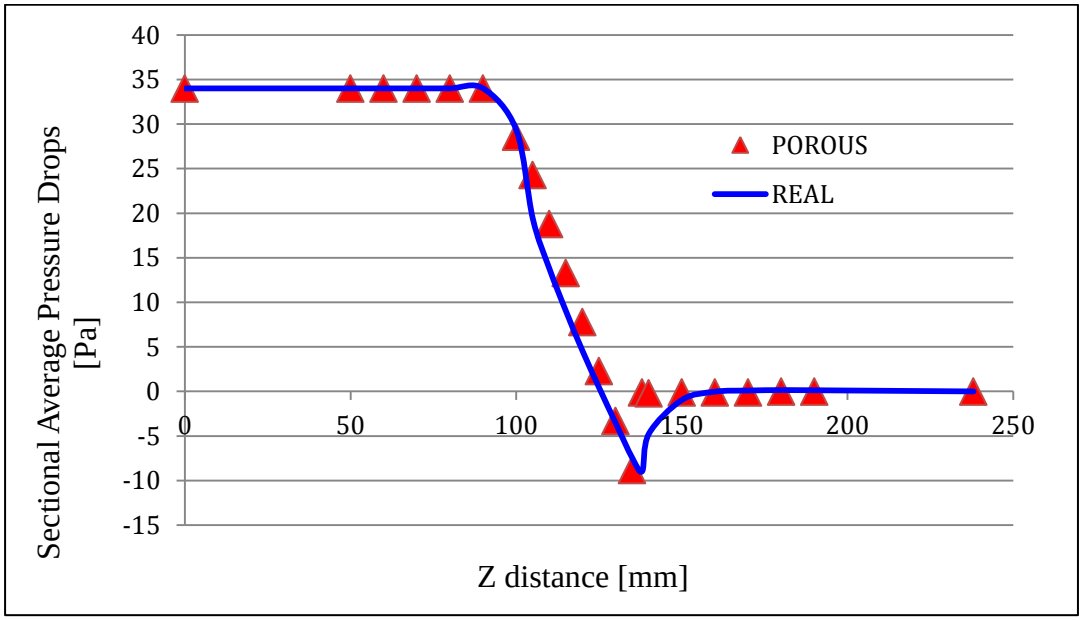

Figure 2.9: Comparison of Sectionally Averaged Pressure Drop for the Physical SF and Porous Medium SF

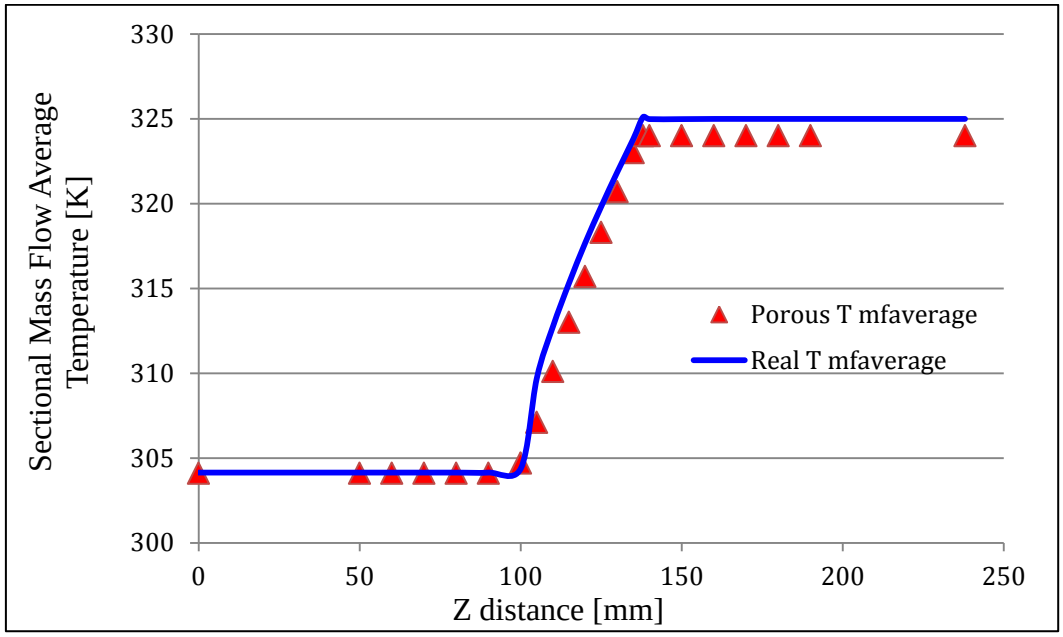

Figure 2.10: Comparison of the Sectionally Mass Flow Averaged Pressure Drop for the Physical SF and Porous Medium SF

According to the presented results, the pressure and temperature drop characteristics are coherent for the physical fin and porous medium. Contour representations for *y*+, velocity and temperature distribution across the fin are presented in Figure 2.11-(a), (b) and (c), respectively:

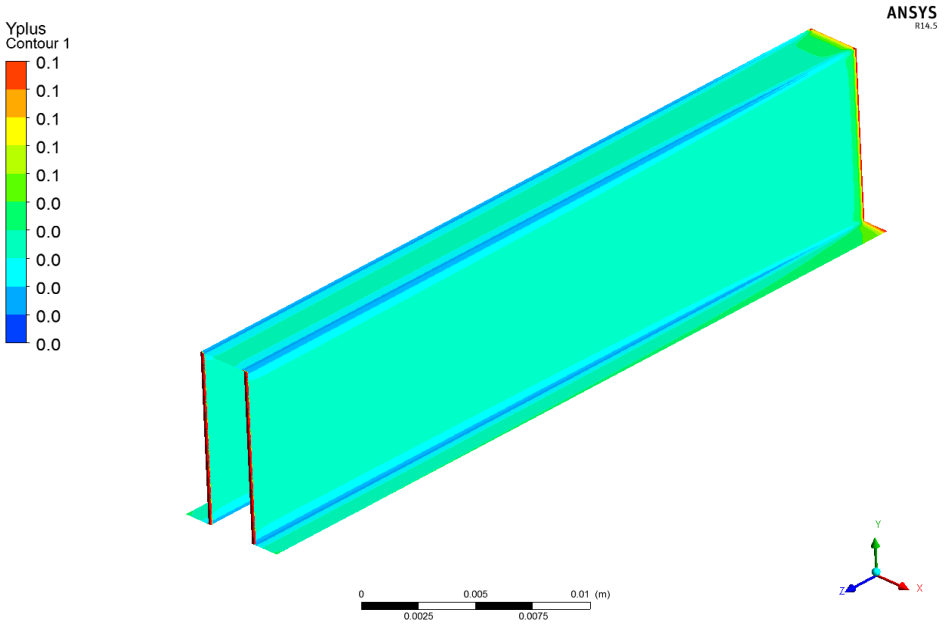

(a)

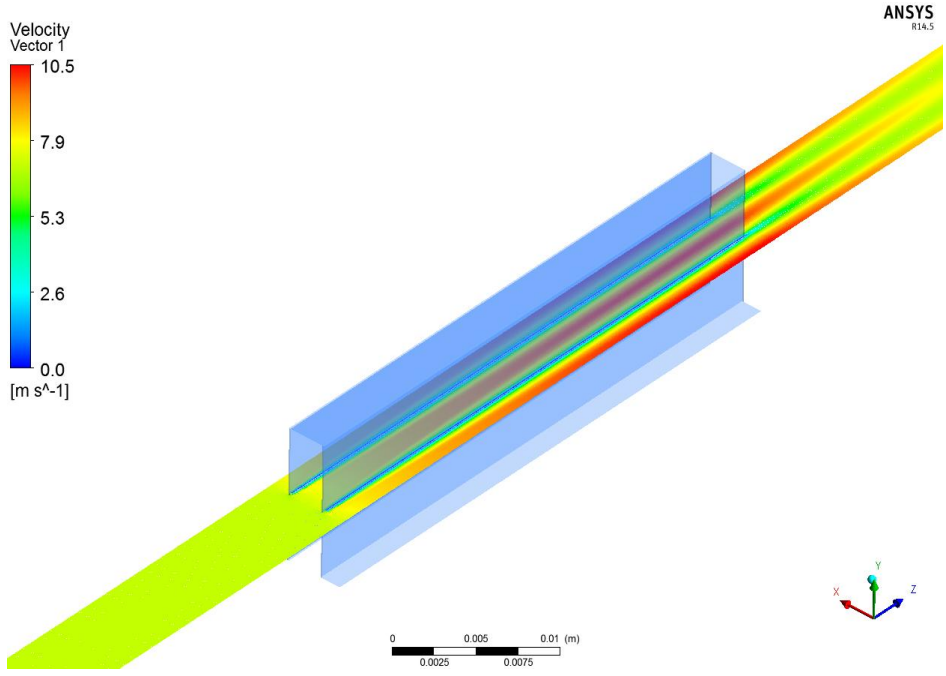

(b)

Figure 2.11: (a) y^+ Contour, (b) Velocity Distribution Across Straight Fin, (c) Temperature Distribution Across Fin

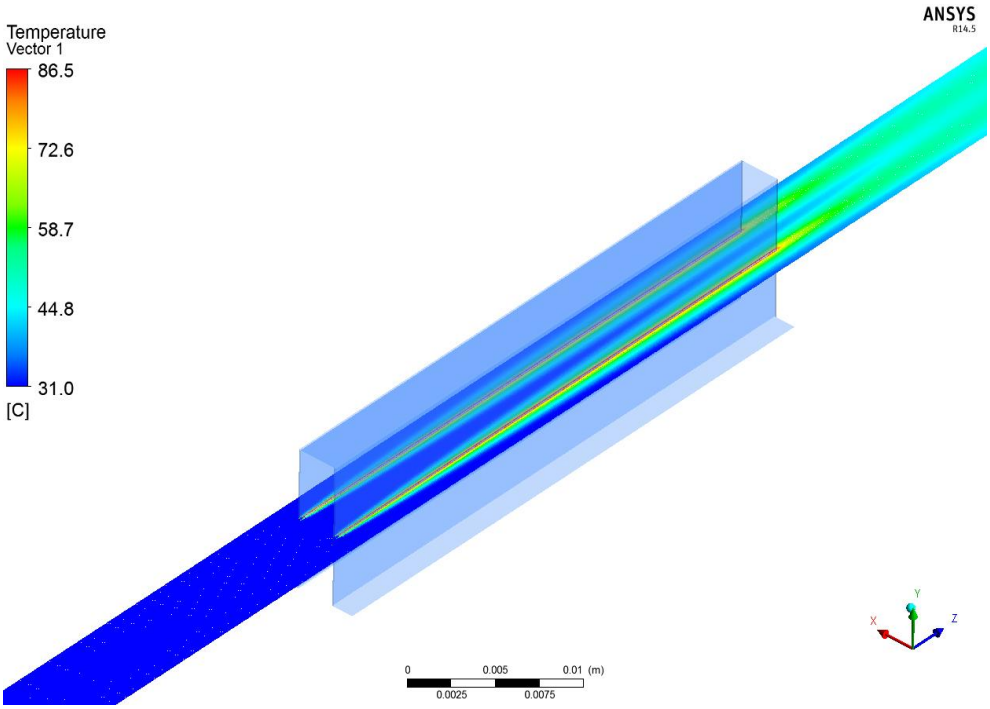

(c)

Figure 2.11: (cont'd)

It is seen from the Model-B results that y^+ value is acceptable with respect to analysis results and velocity and temperature distribution have convenient flow and heat transfer characteristics.

2.3 Wavy Fin Porous Modeling

Wavy fin (WF) structure is used in real life application radiators. Act upon its wavy shape, it provides higher heat transfer rates on radiator. On the other hand, it yields a higher pressure drop across the fin due to its wavy shape. However, this difference is acceptable when considering the heat transfer enhancement characteristics.

The selected wavy fin configuration is 84 mm in length. This type of fin structure is used for 4-row 39-column commercial tractor radiator which is analyzed in Chapter 3.

Similar to the straight fin analysis, the same procedure is followed for the wavy fin. In order to emphasize the simulation process again; firstly physical unit cell wavy fin simulations are analyzed in order to obtain porous medium flow coefficients by using `Forcheimer` relation. Secondly, physical domain with attached upstream and downstream domains is simulated for obtaining the heat transfer parameters and porous jump coefficients. Lastly, porous fin with attached upstream and downstream domains is analyzed with the input parameters that are obtained from physical fin simulations. These simulations are carried out to compare the pressure and temperature drop characteristics across the fin for physical and porous fin simulations. In physical fin model simulations, the exact geometry of the fin is placed in the air stream, while porous domain is located in the stream for porous medium fin model simulations.

2.3.1 Physical Fin Simulations

Unit cell of the wavy fin model, referred to as Model-A (Figure 2.12-(a)), is analyzed in order to obtain porous media characteristics. Model-B, which is a unit cell of the wavy fin with additional upstream and downstream domains as seen in Figure 2.12-(b), is also analyzed. Porous jump boundary conditions are introduced to match the results of the two models.

Boundary conditions for Model-A is set as follows: The velocity inlet and pressure outlet boundary conditions are assigned for the fin inlet and outlet, respectively. Wall boundary condition is applied for the upper and lower walls, while the periodic boundary condition is used for the right and left sides. For Model-B, additional upstream symmetry and downstream symmetry are assigned for upstream and downstream domains.

For both simulations, SIMPLE method is used with least square based cell approximation. Additionally; standard scheme for pressure and the second order upwinding schemes for momentum, turbulent kinetic energy and turbulent dissipation rate are employed. Relaxation factors are set to their default values. For

both simulations, a minimum convergence of $1x10^{-5}$ is obtained for all residuals. For turbulence modeling; k-ε realizable turbulence model with standard wall functions is used.

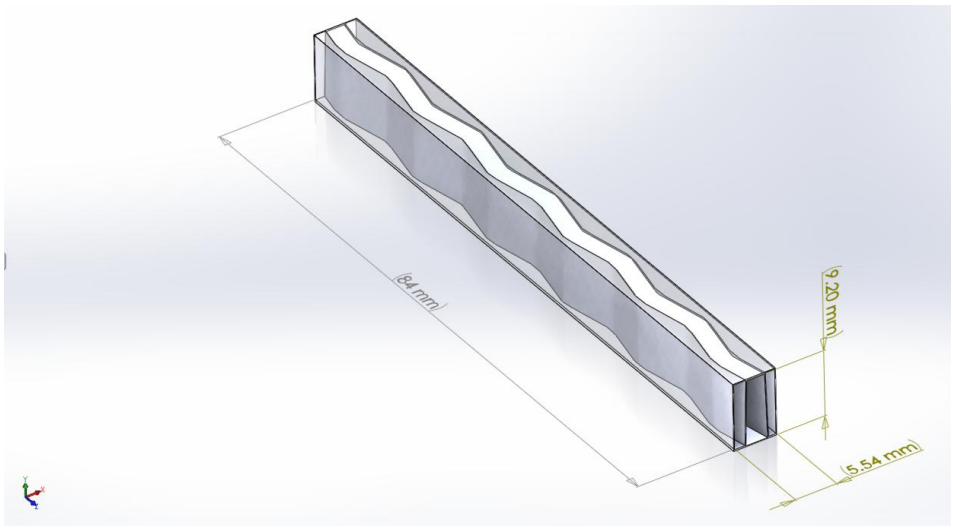

(a)

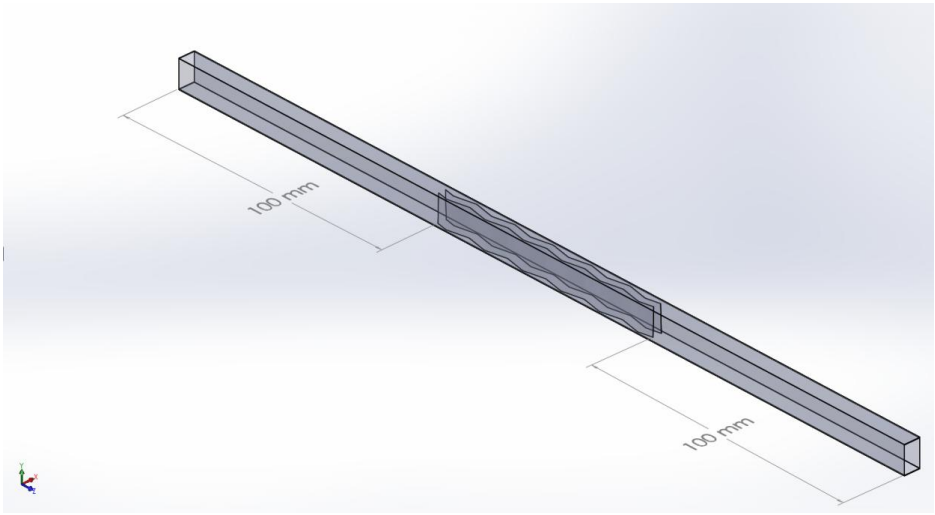

(b)

Figure 2.12: **(a)** Model-A: WF Unit Cell Domain, **(b)** Model-B: WF Unit Cell with Additional Inlet and Exit Domains

2.3.1.1 Mesh Independency

Mesh independency analysis is performed on Model-A. Model-B has thesame geometry unless it has upstream and downstream domain so that selected mesh configuration and sizing parameters for Model-A is also applied to Model-B. Five different mesh configurations are simulated and tetrahedron mesh is used with boundary layer mesh for mesh all configurations. Table 2.6 and Figure 2.13 illustrate the results of the mesh independency studies.

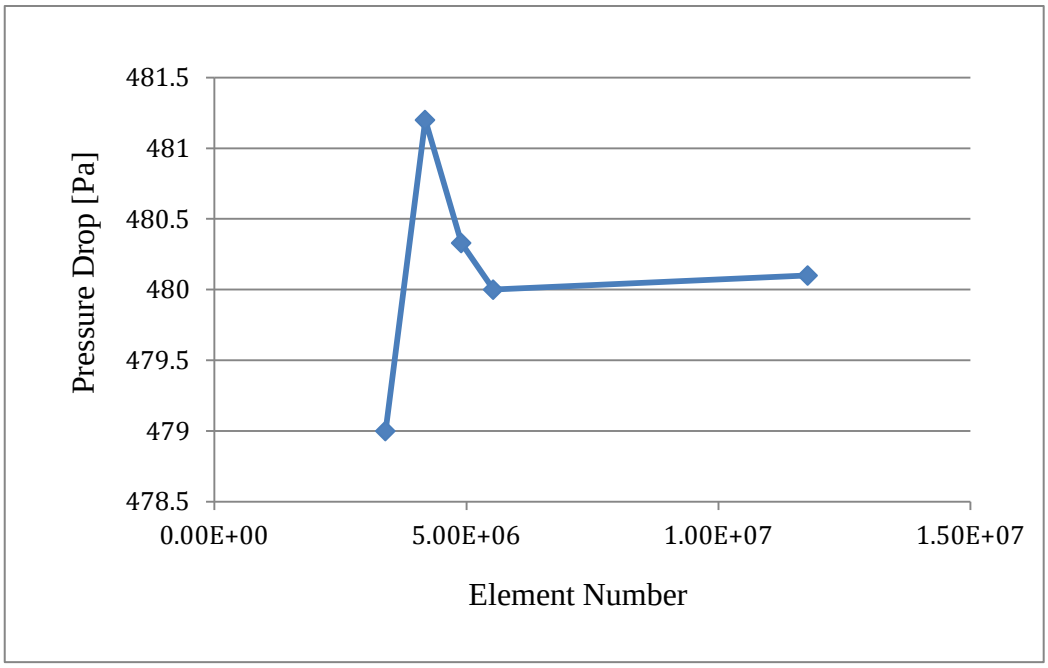

Figure 2.13: Mesh Independency Study for Model-A

Table 2.6: Mesh Independency Analysis

	Element Number	Pressure Drop [Pa]	Skewness
Mesh 1	3,396,616	479.0	0.233
Mesh 2	4,183,300	481.2	0.231
Mesh 3	4,900,713	480.3	0.241
Mesh 4	5,535,117	480.0	0.229
Mesh 5	11,774,387	480.1	0.208

According to the results, the third mesh configuration containing 4,900,713 elements is selected for the Model-A (Figure 2.14-(a)) simulations. With the same mesh parameters, Model-B is meshed and 8,790,703 elements are generated (Figure 2.14-(b)).

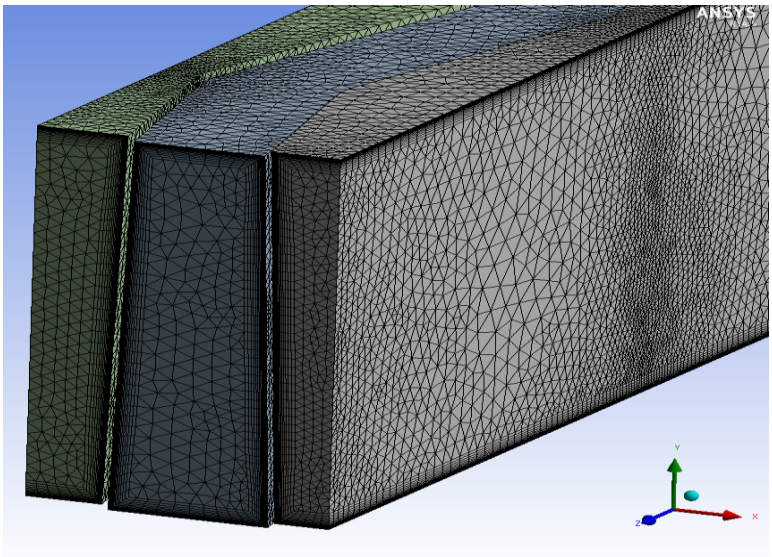

(a)

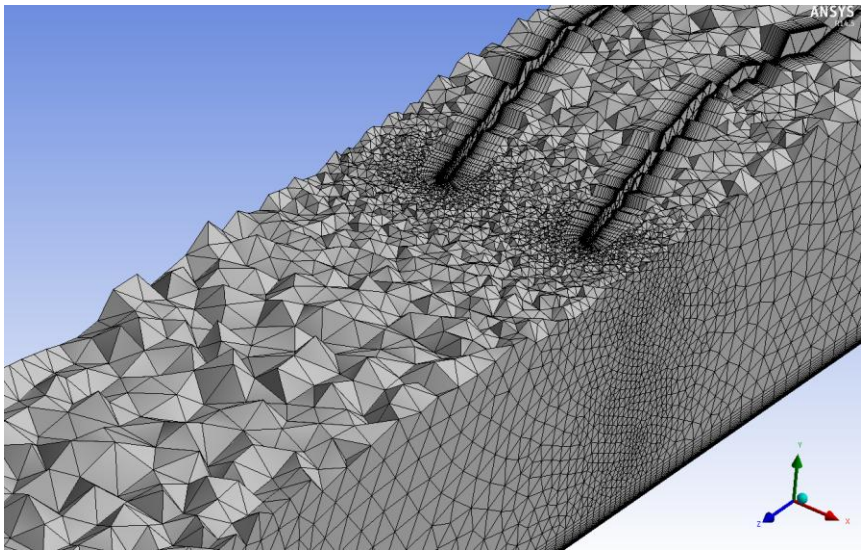

(b)

Figure 2.14: **(a)** WF Model-A Mesh Configuration, **(b)** WF Model-B Mesh Configuration

2.3.1.2 Extraction of Porous Model Parameters

Flow parameters are obtained by using the Forcheimer's relation. Model-A is simulated using different Reynolds numbers and Forcheimer curve is obtained. Table 2.7 contains the input parameters for the Model-A. In Figure 2.15, pressure is plotted against velocity and, and a second order curve was fitted to the simulation data. The corresponding inertial and viscous coefficients are determined to be 17.3 and 4.01×10^{6}, respectively.

Table 2.7: Input Parameters for Unit Cell Wavy Fin Simulations

	Description	Unit
Domain length	84	mm
Element number	4,900,713	
Skewness (average)	0.241	
Turbulence modeling	k-ε-realizable	
Fin volume	2.2567×10^{-7}	m^3
Total volume	4.28131×10^{-6}	m^3
Porosity	0.9473	
Hydraulic diameter	0.00241	m
Turbulence Intensity	0.058	
Turbulence length	0.000169	m
Solution method	SIMPLE	
Computation time / per simulation	30	mins

Heat transfer parameters are obtained from Model-B simulation. For model-B simulation, the input parameters are defined as 7 m/s for the inlet velocity, 304.15 K for the inlet temperature and 359.65 K for the temperature of fin walls. Average surface heat transfer coefficient and tuned porous jump coefficients for the unit cell of a wavy fin are presented in Tables 2.8 and 2.9, respectively.

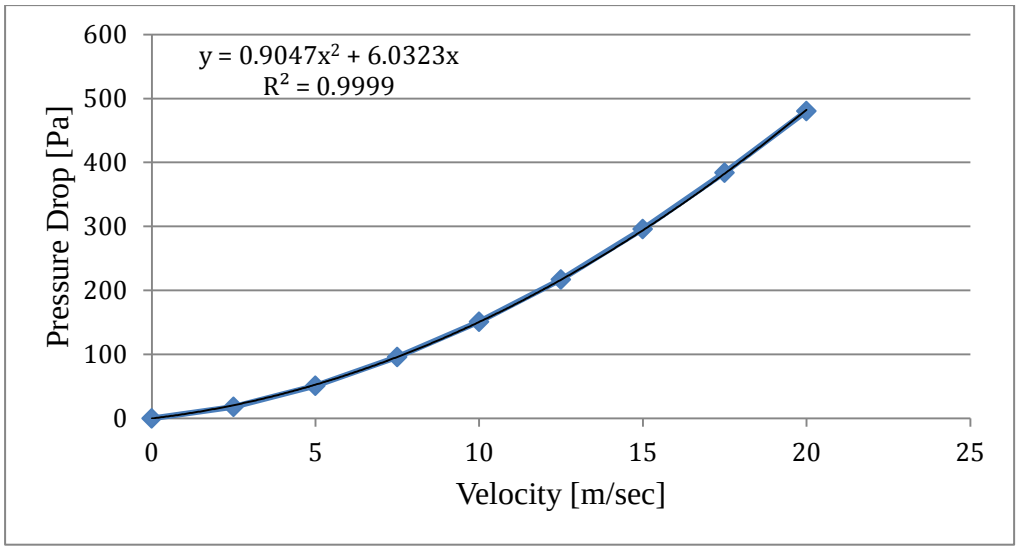

Figure 2.15: Unit Cell Physical WF Simulation Pressure vs. Velocity Plot

Table 2.8: Heat Transfer Characteristics for a Unit Cell of a Wavy Fin

Interfacial area [m^2]	Porous volume [m^3]	IAD [1/m]	HTC [W/m^2-K]	T_{ref} [K]
0.003957696	4.28131×10^{-6}	810	170	336

Table 2.9: Porous Jump Coefficients for a Unit Cell of a Wavy Fin

	Face permeability [$1/m^2$]	Thickness [m]	Inertial coefficient [1/m]
Inlet	4.01×10^6	0.1	3.42
Outlet	4.01×10^6	0.1	-5.2

2.3.2 Wavy Fin Simulations with Porous Modeling

Similar to the physical fin simulations, porous fin simulations are conducted by using the same process. However, in this case, simulations are conducted only under unit cell of the porous wavy fin domain with additionally attached upstream and

downstream domains as seen in Figure 2.16-(a). Afterwards, a comparison is made between this model and Model-B of physical fins.

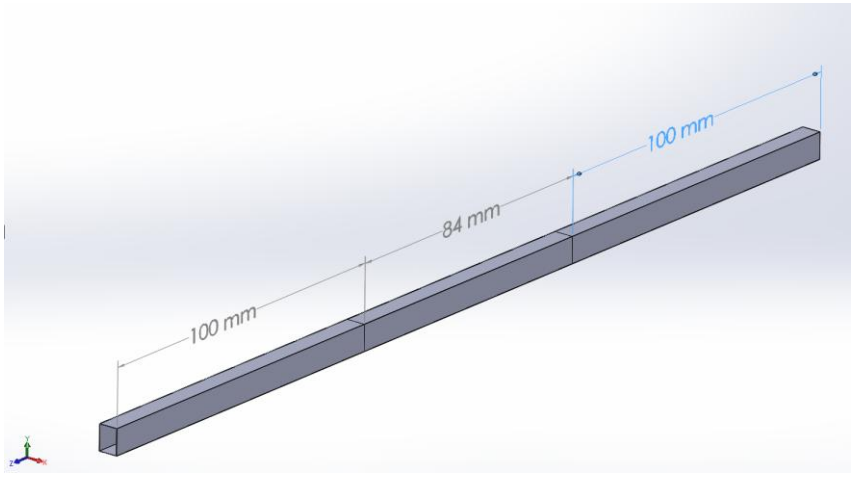

(a)

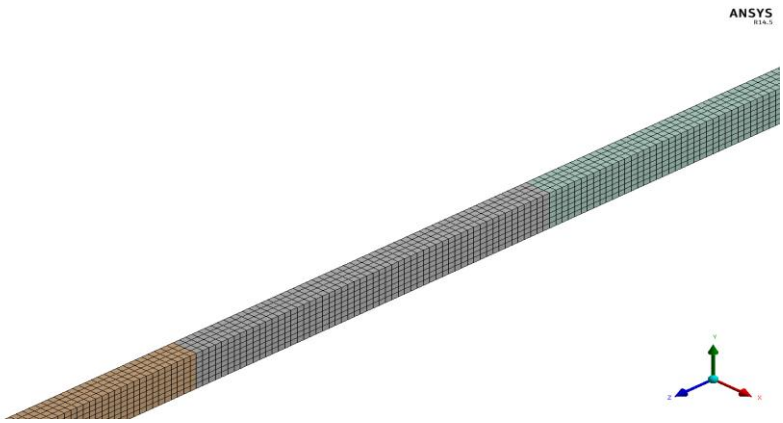

(b)

Figure 2.16: **(a)** Unit Cell Porous WF with Additional Inlet and Exit Domain **(b)** Mesh Configuration

For the porous fin model, hexa-sweep meshing was used. The mesh of the porous model (Figure 2.16-(b)) consists of 5,320 elements with a skewness of 4.89×10^{-7}. After completing the meshing process, boundary conditions are assigned. Besides the physical fin boundary condition configurations, additional porous jump boundary conditions were assigned to inlet and outlet of the porous domain as the porous medium boundary conditions, All FLUENT solver settings are taken to be the same as the physical fin simulations.

2.3.3 Comparison and Discussion

After porous medium flow coefficients, porous jump coefficients and heat transfer parameters are obtained from the simulation of a unit cell of a wavy physical fin, porous medium simulations are carried out with the same input parameters and comparison is made. Figure 2.17 compares the sectionally averaged pressure drop for the physical fin and porous medium. Figure 2.18 shows the same comparison for the sectional mass flow averaged temperature drop.

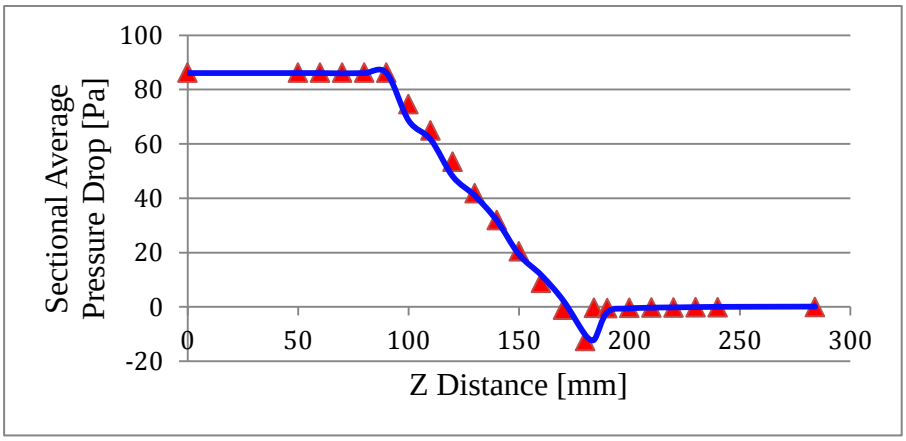

Figure 2.17: Sectionally Averaged Pressure Drop Comparison of the Physical WF and Porous Medium WF

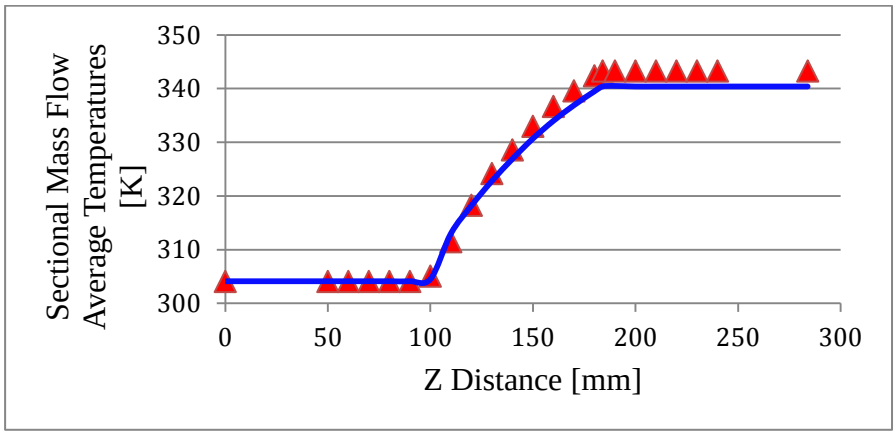

Figure 2.18: Sectionally Mass Flow Averaged Temperature Drop Comparison of the Physical WF and Porous Medium WF

According to the presented results, pressure and temperature drop characteristics are coherent between the physical fin and porous medium. Contour representations for *y*+, velocity and temperature distribution across the fin are presented in Figures 2.19-(a), (b) and (c), respectively:

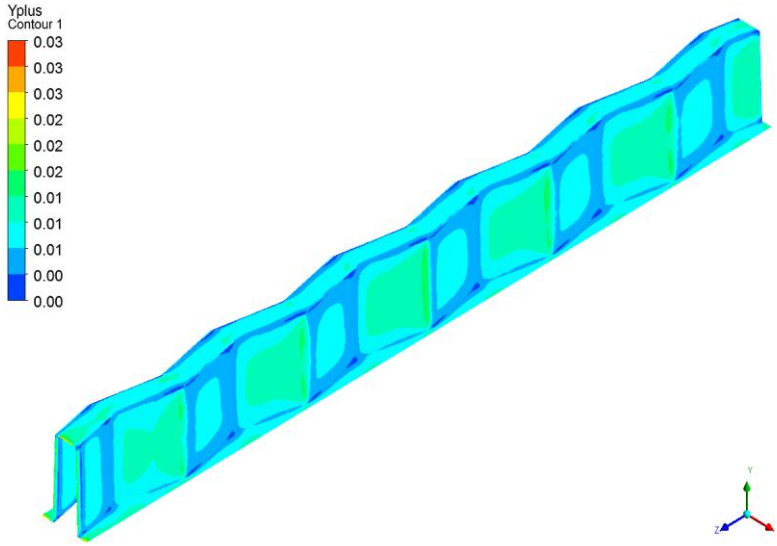

(a)

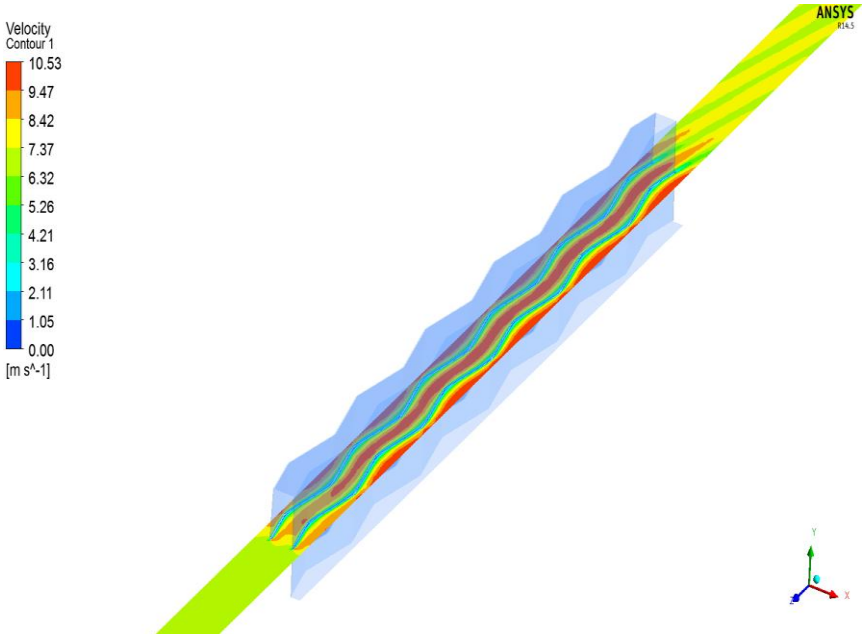

(b)

Figure 2.19: (a) y^+ contour, (b) Velocity Distribution Across WF, (c) Temperature Distribution Across WF

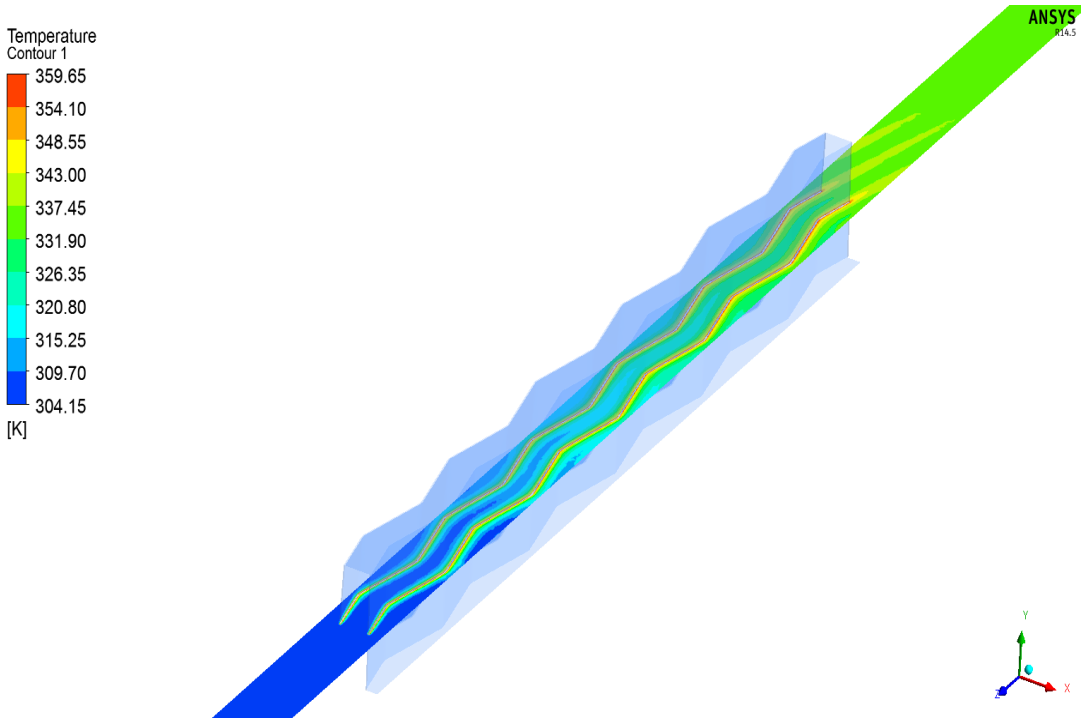

(c)

Figure 2.19: (cont'd)

It is seen from the Model-B results that $y+$ value is acceptable with respect to analysis results and velocity and temperature distribution has convenient characteristics.

2.4 Concluding Remarks

Up to now, porous modeling analysis has been conducted on the straight fin and wavy fin configurations. Porous medium flow, heat transfer and porous jump coefficients are obtained for the full-sized radiator analysis. In the next chapter, the full-sized radiator analysis for 2-rows 10-columns and 4-row 39-column radiators will be presented.

CHAPTER 3

COMPUTATIONAL MODELING

After obtaining the input parameters for fluid flow and heat transfer for the porous medium, full-sized radiator models containing 2-row 10-column (20-tubed) and 4-row 39-column (156-tubed) were prepared. 38 mm straight fin is used for 2-row 10-column radiator and 84 mm wavy fin is used for 4-row 39-column radiator. Porous medium flow and heat transfer parameters that are obtained in Chapter 2 are used in the air-side (fin-side) of the full-sized radiators as input parameters. Water-side of the radiator is modeled as a regular fluid domain. Continuity, momentum and energy equations for water-side are governed by equations (3.1)-(3.3) [3]:

$$\frac{\partial \rho}{\partial t} + \nabla.(\rho\,\vec{v}) = 0 \tag{3.1}$$

$$\frac{\partial}{\partial t}(\rho\vec{v}) + \nabla.(\rho\vec{v}\vec{v}) = -\nabla p + \nabla.(\bar{\bar{\tau}}) + \rho\vec{g} + \vec{F} \tag{3.2}$$

where p is static pressure, $\bar{\bar{\tau}}$ is stress tensor $\rho\vec{g}$ is gravitational body force and $\vec{F}$ is external body force. $\bar{\bar{\tau}}$ is given as follows:

$$\bar{\bar{\tau}} = \mu\left[\left(\nabla\vec{v} + \nabla\vec{v}^{T}\right) - \frac{2}{3}\nabla.\vec{v}\,I\right)\right] \tag{3.3}$$

where μ is the molecular viscosity and I is the unit tensor.

$$\frac{\partial}{\partial t}(\rho E) + \nabla.\left(\vec{v}(\rho E + p)\right) = \nabla.\left(k_{eff}\nabla T - \sum_{j} h_j\vec{J}_j + \left(\overline{\overline{\tau_{eff}}}.\vec{v}\right)\right) + S_h \tag{3.4}$$

where k_{eff} is effective conductivity, $\vec{J}_j$ is the diffusion flux and S_h is the heat source. E is defined as;

$$E = h - \frac{p}{\rho} + \frac{v^2}{2} \tag{3.5}$$

where h is sensible enthalpy.

3.1 Modeling of 2-Row 10-Column Radiator

2-row 10-column radiator is a prototype model. Due to the high mesh requirements of full-sized radiator models, it is convenient to start with a small scale radiator model. Since the problem consists of two fluid domains with conjugate heat transfer between the domains, the adversities during the pre-processing and solving stages are clearly revealed with the aid of this small scale model. The analysis of the 4-row 39-column radiator is then carried out with the same procedure due to the similarity between the two radiators.

To start with, a 3-D CAD model of the radiator is formed by using commercial CAD software. 3-D CAD model of the 2-row 10-column radiator is presented in Figure 3.1 with the necessary dimensions. Model consists of upstream, downstream, fin and water domains. The upstream domain simulates the free stream air which represents the pressurized air coming from the fan or front grill of the vehicle, while the downstream domain describes the outflow air leaving the radiator. Tube thickness was neglected during the 3-D modeling in order to make convenience in meshing part.

During the meshing process fin, upstream, downstream and tube domains were meshed with hexa-type elements; while the upper and lower tanks were meshed with tetra elements, and these meshes were coupled with each other. To match the meshes of the upper and lower tanks with the mesh of the tubes, it is necessary to select the thickness of the first layer of the boundary layer mesh on the tube walls as 0.1 mm. It

was also observed that the number of boundary layer meshes does not affect the flow field significantly. Therefore, in order to keep the number of meshes in a reasonable level, tubes were meshed with a boundary layer mesh having 2 layers with 0.1 mm first layer height. The generated mesh (Figure 3.2) consists of 9,417,705 elements with an average skewness value of 0.184.

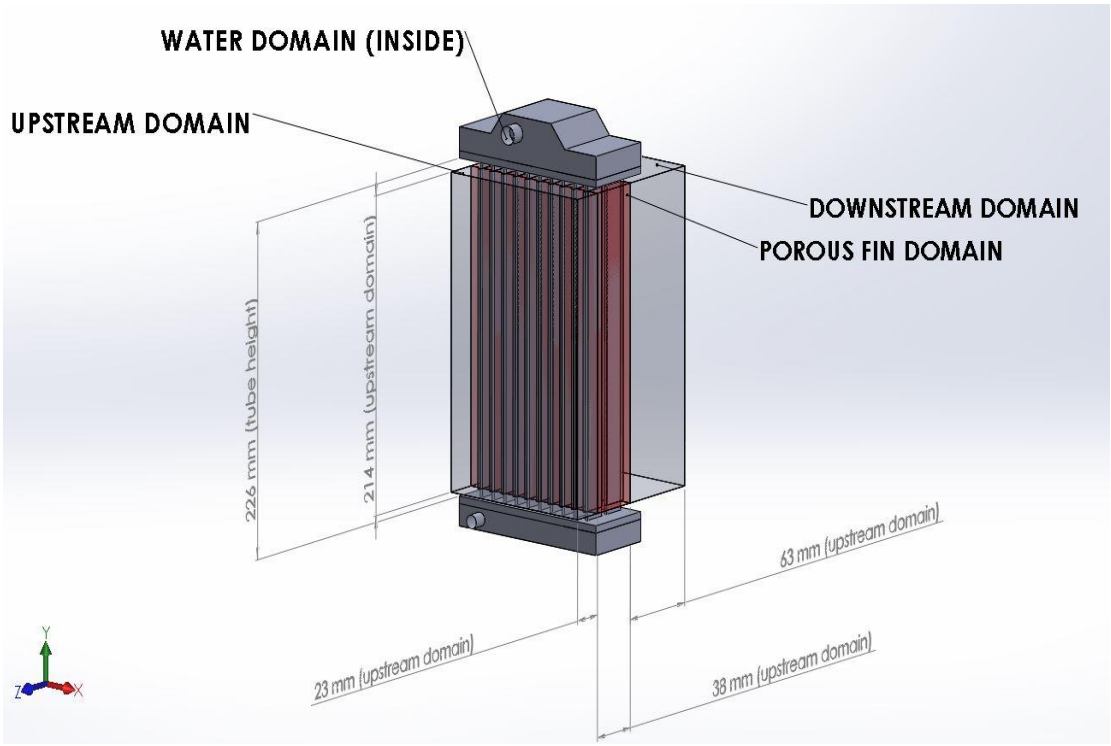

Figure 3.1: 2-row 10-column Radiator

During the porous modeling in FLUENT® coupling upstream, downstream, fin and tube domains needs to coupled appropriately. Special attention should be given to this coupling due to the dual porous zone approach used in FLUENT®. In pre-processing part of the modeling, with the use of non-equilibrium thermal model for the porous fin side, FLUENT® creates another coincident imaginary domain besides the fluid domain inside the fin in order to analyze both fluid and solid parts of the porous fin medium. Due to the internal limitations of dual porous zone approach used in FLUENT® imaginary solid and fluid porous domains cannot be coupled with the tube domains at the same time. For this reason, the imaginary solid domain is coupled with the tube domain to model heat transfer between the fins and the fluid.

While modeling fluid flow, imaginary solid domain is not considered, and the fluid domain is coupled with the tube domains. Moreover, the fluid domain is also coupled with the upstream and downstream domains. All the couplings are performed by using the text user interface (TUI) commands of FLUENT®.

Mass flow inlet, pressure outlet, velocity inlet, pressure outlet, upstream wall and downstream wall boundary conditions were assigned for water inlet, water outlet, air inlet, air outlet, upstream domain boundary and downstream domain boundary, respectively. The air inlet velocity is taken as 7 m/s with a temperature of 304.2 K temperature, while the mass flow rate of water is 0.309 kg/s with an inlet temperature of 359.7 K. Fluid flow, heat transfer and porous jump parameters for the porous medium are taken from Section 2.2 of Chapter 2.

In FLUENT, second order upwind scheme was used for momentum, turbulent kinetic energy (TKE) and turbulent dissipation rate (TDR). Relaxation factors are selected as 0.05 for momentum, 0.3 for TKE and TDR and 0.4 for turbulent viscosity in order to obtain optimized convergence rate and solution time.

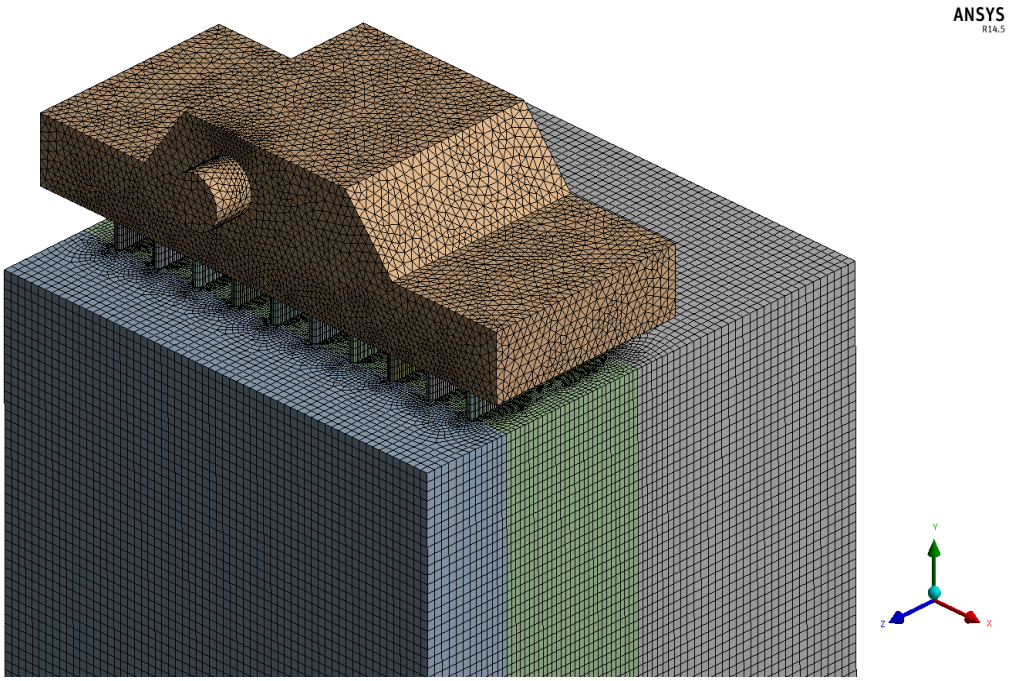

Figure 3.2: Mesh for the 2-row 10-column Radiator

Finally, the simulation of 2-row 10-column model radiator was performed. Input parameters and boundary conditions for this simulation are presented in Table 3.1. A converged solution was obtained after 426 iterations when the minimum residual was smaller than $1x10^{-4}$. The simulations were performed on a DELL T5600 Workstation (Intel® Xeon®, 3.30 GHz, 2 processors, 16 cores, 128 RAM). The overall solution time was approximately 3 hours and 12 minutes.

Table 3.1: Input Parameters for the Simulation of a 2x10 Tube Radiator

Inlet air velocity [m/s]	Inlet water mass flow rate [kg/sec]	Heat transfer coefficient [W/m^2K]	Interfacial area density [1/m]	Water inlet temperature [K]	Air inlet temperature [K]
7	0.309	133	809	359.65	304.14

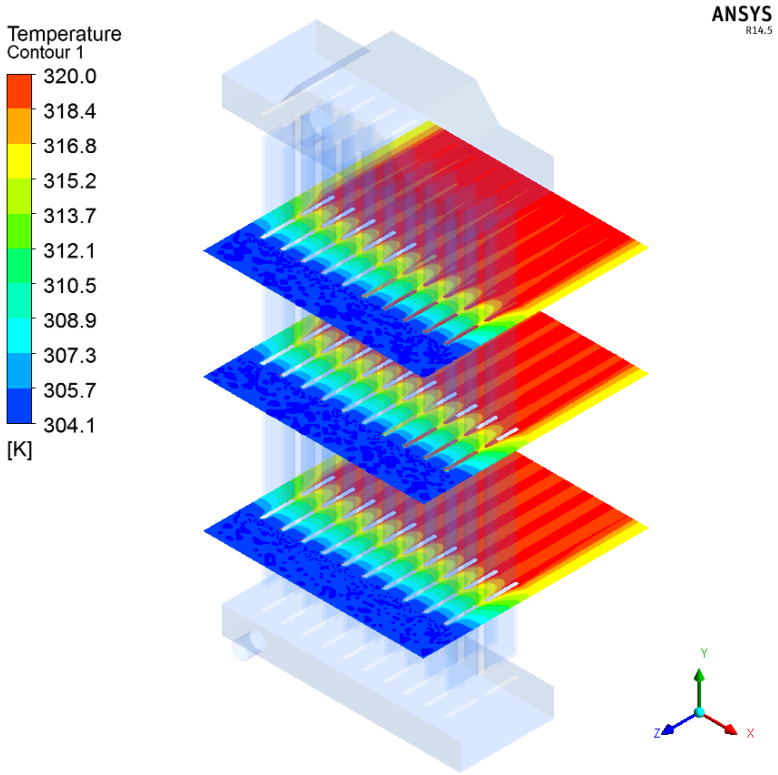

Figure 3.3: Air-side Temperature Distribution

Cross-sectional temperature distribution for the air-side and streamlines colored by temperature at water side are presented in Figures 3.3 and 3.4, respectively. Temperature gradients are achieved in *z* and *y*-directions as expected. Air-side has an increasing temperature in the flow direction as a result of the heat transfer from the water-side. On the other hand, water-side has a decreasing temperature in the flow direction. According to the simulation, the average outlet water temperature was found to be 356.9 K. As a result, total water temperature drop across the radiator was 2.75 K. According to this temperature drop, the total heat capacity of the radiator was calculated as;

$$Q = \dot{m}\, C_p\, \Delta T = 0.309\ x\ 4208\ x\ 2.75 = 3{,}585\ W \tag{3.6}$$

The pressure drop for water which is also an important performance parameter for radiators was found to be 2.21 kPa.

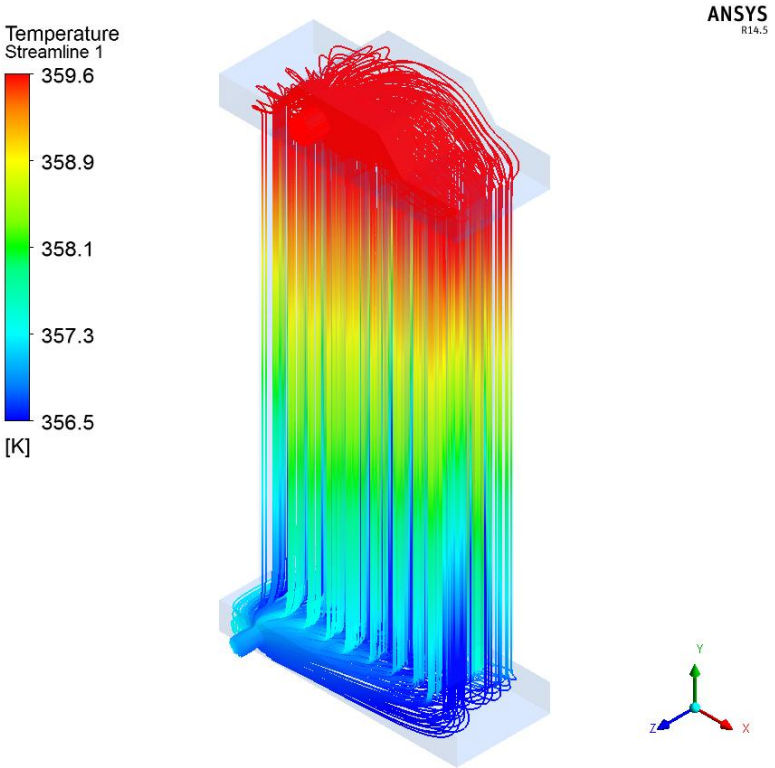

Figure 3.4: Water-side Streamlines Colored According to the Temperature

Additionally, water-side streamlines colored by velocity are presented in Figure 3.5. As seen from the figure, the flow is not among the tubes which affect the thermal characteristics of the radiator. Moreover, the flow is concentrated around the exit nozzle due to its location in the lower tank.

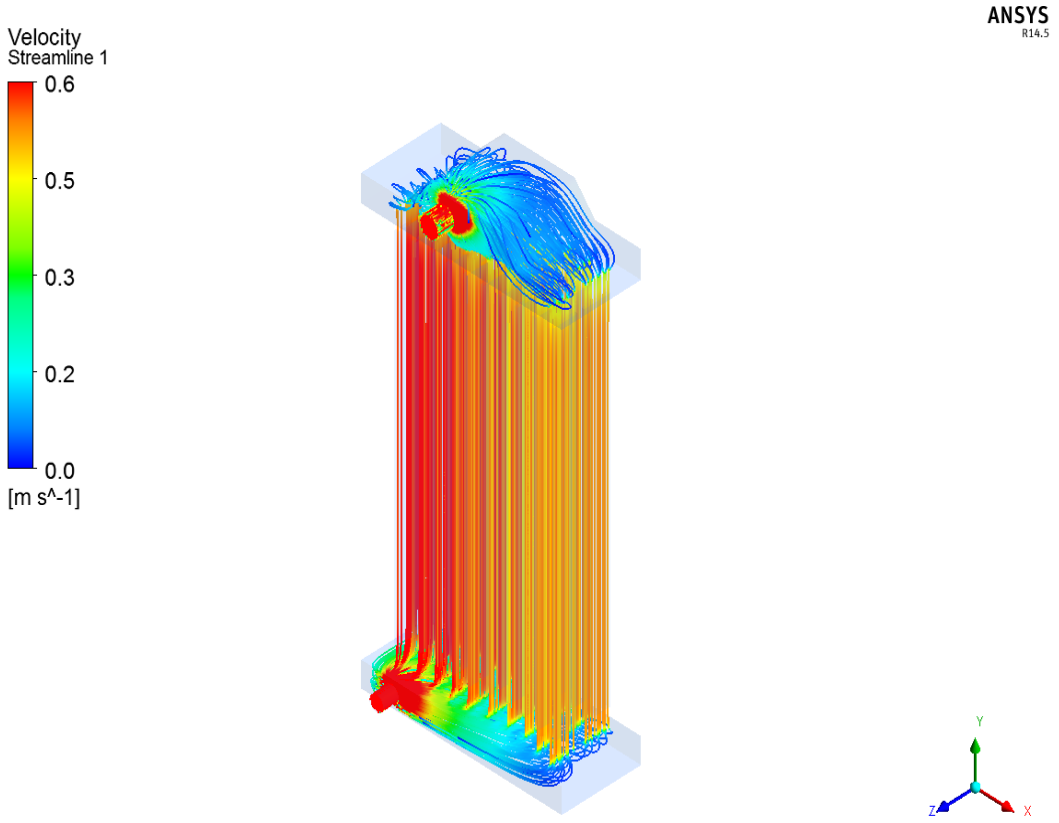

Figure 3.5: Water-side Streamlines Colored According to the Velocity

3.2 Modeling of 4-Row 39-Column Radiator

The 4-row 39-column radiator is manufactured for an anonymous tractor company. Tractor has 64 HP Perkins engine which requires a minimum cooling capacity of 55 kW according to the catalog data. The thermal performance of this radiator was obtained as 55,8 kW with the in-house experiments by the tractor company. Catalog data are tabulated in Table 3.2.

Similar to the 2-row 10-column radiator, 3-D CAD model of the 4-row 39-column radiator is prepared by using the same commercial CAD software. Figures 3.6-(a) and (b) present the 3-D CAD model with the necessary dimensions. After forming the 3-D model, meshing process was progressed. Fin, upstream, downstream and tube domains were meshed with hexa-type elements; while the upper and lower tanks were meshed with tetra elements and these meshes were coupled with each other. Tubes were meshed with a boundary layer mesh having 2 layers with 0.1 mm first layer height. The generated mesh (Figure 3.7) consists of 53,355,356 elements with an average skewness value of 0.178. Coupling between upstream, downstream, fluid fin, solid fin and tubes were performed with the same procedure as it is described in section 3.1.

Table 3.2: Experimental Data for 4-row 39-column Radiator

Definition	Value
Rotational speed of engine [rpm]	2,200
Inlet temperature [^{o}C]	86.5
Outlet temperature [^{o}C]	81
Ambient temperature [^{o}C]	31
Inlet mass flow rate [kg/sec]	2.41
Air velocity [m/sec]	7
Heat rejection [kW]	55.8

Mass flow inlet, pressure outlet, velocity inlet, pressure outlet, upstream wall and downstream wall boundary conditions were assigned for water inlet, water outlet, air inlet, air outlet, upstream domain boundary and downstream domain boundary, respectively. The air inlet velocity is taken as 7 m/s with a temperature of 304.2 K temperature, while the mass flow rate of water is 2.41 kg/s with an inlet temperature of 359.7 K. Fluid flow, heat transfer and porous jump input parameters for the porous medium are taken from Section 2.3.

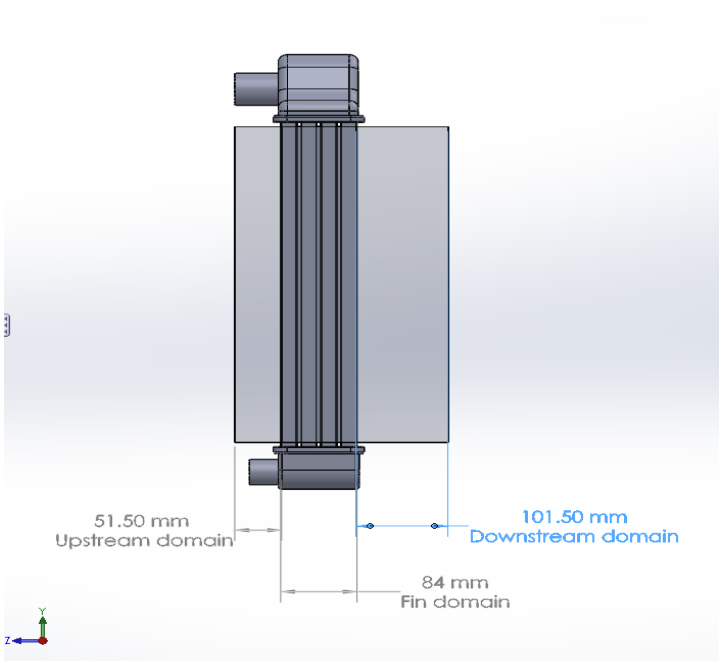

(a)

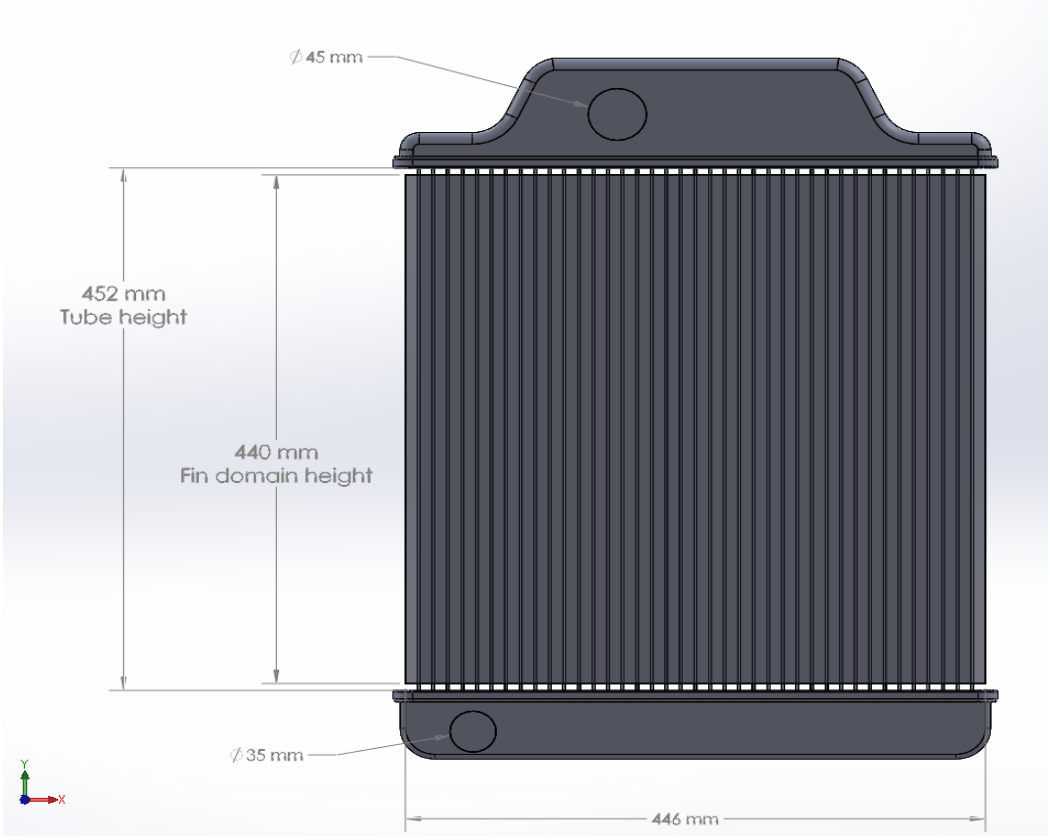

(b)

Figure 3.6: 4-row 39-column Radiator CAD Model, (a) Front View, (b) Right View

In FLUENT®, second order upwind scheme was used for momentum, turbulent kinetic energy (TKE) and turbulent dissipation rate (TDR). Relaxation factors are selected as 0.05 for momentum, 0.3 for TKE and TDR and 0.4 for turbulent viscosity in order to obtain optimized convergence rate and solution time.

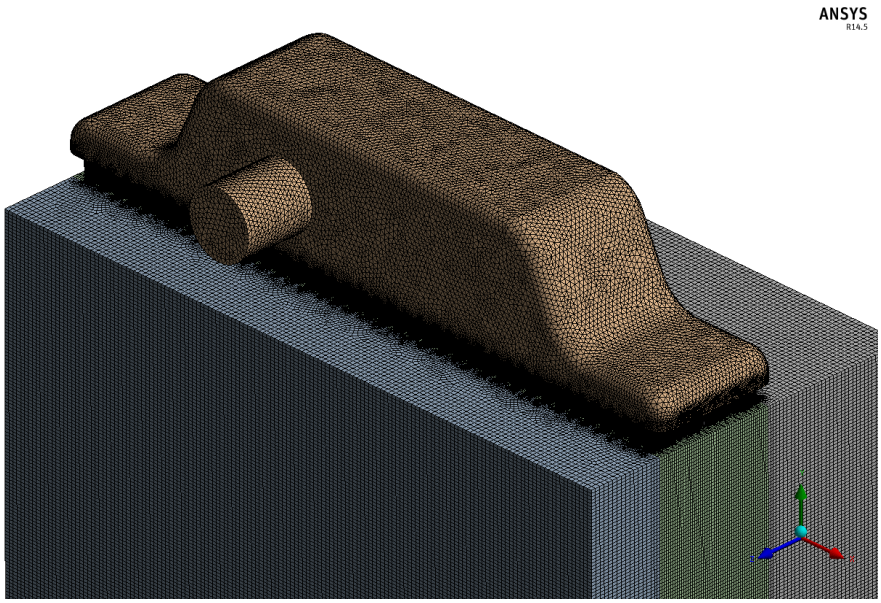

Figure 3.7: Mesh for the 2-row 10-column Model Radiator

The analysis of 4-row 39 column radiator is performed by using the input parameters that are presented in Table 3.3. A converged solution was obtained after 472 iterations when the minimum residual was smaller than $1x10^{-4}$. The simulations were performed on a DELL T5600 Workstation (Intel® Xeon®, 3.30 Ghz, 2 processors, 16 cores, 128 RAM). The overall solution time was approximately 12 hours and 40 minutes.

Table 3.3: Input Parameters for the Simulation of a 2x10 Tube Radiator

Inlet air velocity [m/s]	Inlet water mass flow rate [kg/s]	Heat transfer coefficient [W/m^{2}K]	Interfacial area density [1/m]	Water inlet temperature [K]	Air inlet temperature [K]
7	2.41	170	810	359.65	304.14

Cross-sectional temperature distribution, velocity distribution for the air-side, and water side streamlines colored by temperature and water side streamlines colored by velocity are presented in Figures 3.8, 3.9, 3.10 and 3.11 respectively. Likewise in 2-row 10-column radiator, temperature gradients are successfully achieved in *z* and *y*-directions as expected for 4-row 39-column radiator. Air-side temperature is increasing in the flow direction as a result of the heat transfer from the water-side, while, the water-side temperature is decreasing in the flow direction.

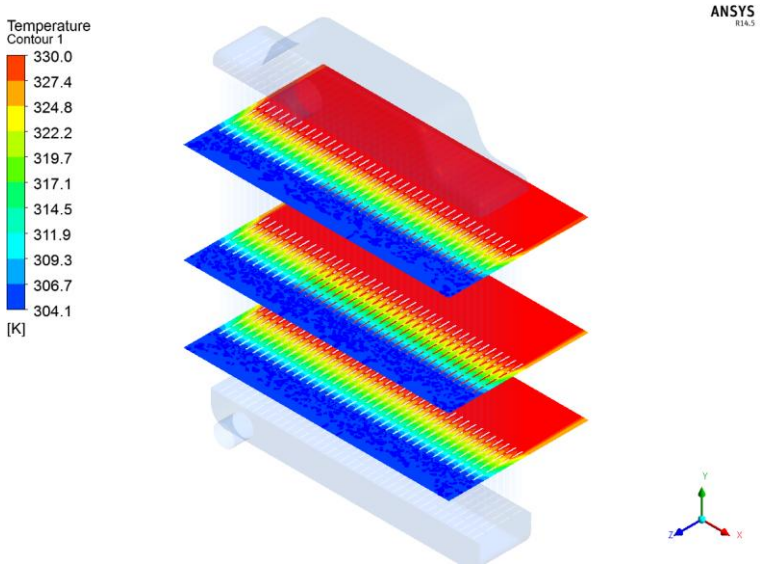

Figure 3.8: Air-side Temperature Distribution

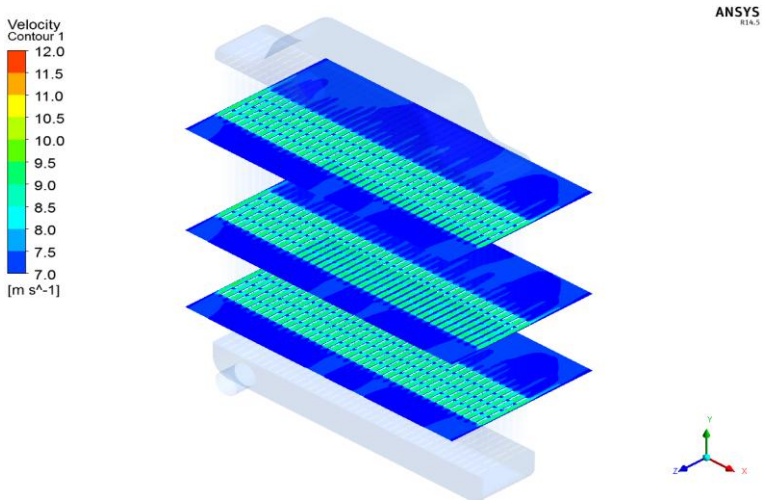

Figure 3.9: Air-side Velocity Distribution

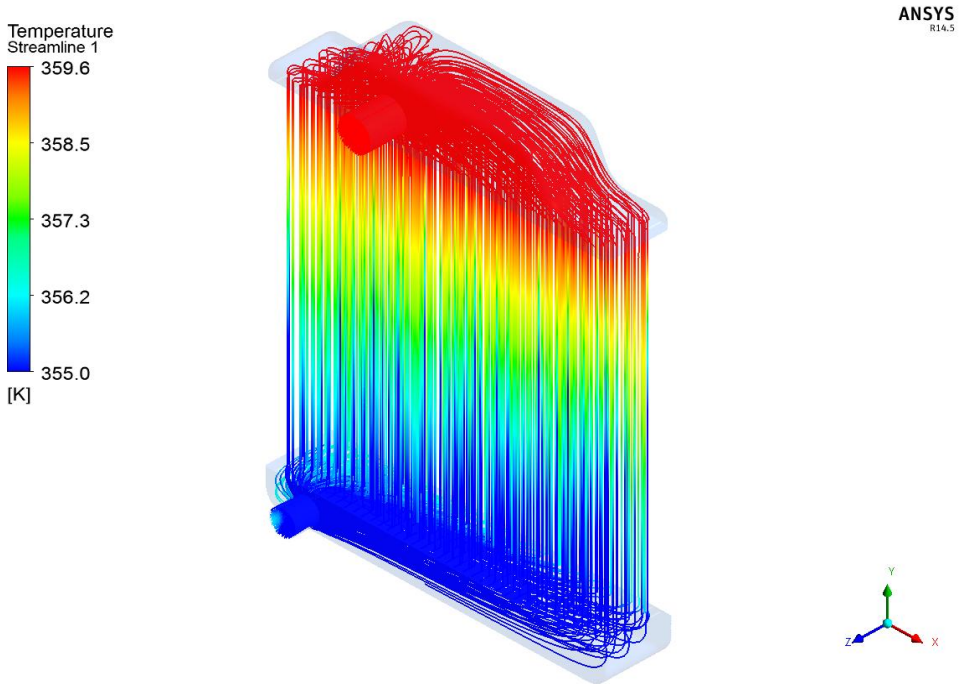

Figure 3.10: Water-side Streamlines Colored According to the Temperature

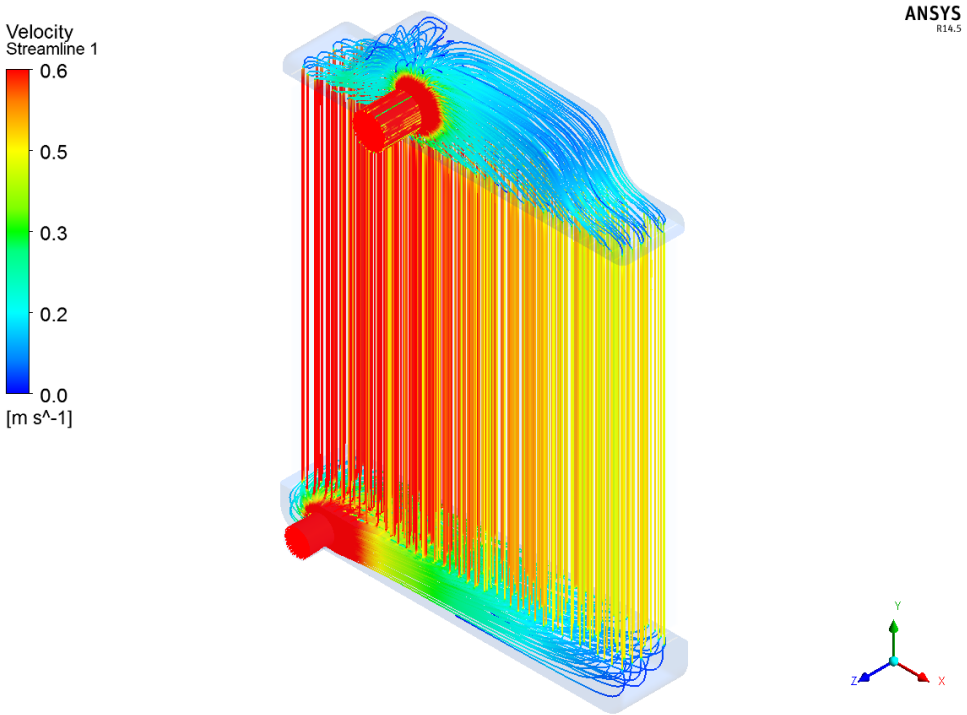

Figure 3.11: Water-side Streamlines Colored According to the Velocity

As discussed for the small scale radiator, again the flow is not distributed among tubes as seen in Figure 3.11. This non-uniformity also contributes to the temperature gradient among the tubes in the x-direction. According to the simulation, the average outlet water temperature was found to be 354.3 K. As a result, total temperature drop of water through the radiator was 5.36 K. According to this temperature drop, the total heat capacity of the radiator was calculated as;

$$Q = \dot{m}\, C_p\, \Delta T = 2.41\ x\ 4208\ x\ 5.36 = 54{,}413\ W \tag{3.7}$$

The pressure drop for water which is also an important performance parameter for radiators was found to be 6.5 kPa. According to the results, heat transfer and fluid flow characteristics are obtained as expected and the conjugate heat transfer between the domains is substantiated.

3.3 Concluding Remarks

Full-sized 2-row 10-column and 4-row 39-column radiator analysis was performed and results were obtained. 2-row 10-column radiator is nearly half sized with respect to the 4-row 39-column radiator by means of height length.

According to the experimental results for 4-row 39 column radiator, the outlet water temperature is determined as 354.2 K experimentally, while the CFD analysis revealed the same temperature as 354.3 K. There is an error of 2.5 percent between the experimentally and numerically determined outlet water temperatures, which is quite acceptable. The heat capacity of the radiator is determined as 55.8 kW, while it is calculated 54.4 kW in the CFD analysis.

CHAPTER 4

CONCLUSION

In this study, a full-sized vehicle radiator is analyzed by using porous medium approach. Two-equation model is implemented for modeling the heat transfer between the fins and air which is not available in the literature to the best of author's knowledge. Modeling radiator with porous medium approach decreases the computational cost dramatically and leads the way to obtain hydrodynamic and thermal performance of a fin-and-tube type radiator by using CFD analysis. By using this methodology, the thermal performance of a complete radiator design can be obtained within a reasonable computational time and a CFD model with the proposed methodology can be implemented as a design tool for the radiator design which would lead to more optimized radiator designs. Full-sized 2-row 10-column and 4-row 39-column radiator hydrodynamic and thermal analyses were performed by using developed porous modeling.

Porous medium flow and heat transfer characteristics were obtained for straight and wavy type of fin structures. In the literature, generally flow coefficients were obtained by using experimental pressure drop data. However, in this study flow and heat transfer coefficients were obtained from the unit cell fin models which were presented in Chapter 2 (Model-A and Model-B for straight and wavy fin). Porous coefficients were obtained from the analysis of unit cell fin Model-A. Model-A simulations were performed with variable inlet velocities repeatedly and pressure drop data were tabulated with respect to corresponding inlet velocities. It is important to set the upper limit of the inlet velocity higher than the twice of the ideal working velocity, and perform the simulations thru that upper inlet velocity limit leads the way to obtain more accurate porous medium flow characteristics when

compared with the physical fin. For both straight and wavy fin models presented in Chapter 2, according to the pressure and temperature drop characteristics comparison of porous medium and physical fin Model-B, it was seen that results were well-matched with each other. From this conclusion, used computational methodology is a robust and useful tool for determination of porous medium flow and heat transfer coefficients for fin structures. Nevertheless, pressure drop data obtained from Model-A physical fin simulations should be validated with the experimental results.

Full-sized radiator models; 2-row 10-column using straight fin and commercial radiator 4-row 39-column using wavy fin, were analyzed. Commercial 4-row 39-column radiator results were validated with the experimental catalog values of the radiator. Results show that succeeding compatibility was obtained between experimental catalog values and CFD analysis. Experimental value of the radiator is obtained as 55.8 kW while CFD analysis results predicted 54.4 kW watts. % 2.4 of error was calculated between the computational results and the catalog value. Moreover, CFD analysis results illustrate the velocity and temperature distribution in the radiator so that flow and heat transfer characteristics of the radiator can be observed extensively. These visualizations reveals the design flaws and brings important contributions for designing process.

CFD analysis of radiator by using porous medium approach gives reasonable and reliable results. By using CFD analysis, design cost may be decreased dramatically by easing the experimental testing process. Moreover, CFD modeling of a radiator by using porous medium approach is convenient and effective design tool for a radiator. By predicting the velocity and temperature distribution, hydrodynamic and thermal optimization of radiators can be performed.

As a future work, further CFD studies can be performed with different types of radiator configurations and validations can be performed with experimentation Optimization of radiators in terms of size and weight can be performed computationally for a range of cooling capacities. Moreover, fan of the radiator may be implemented into the computational model for more realistic studies especially

for other vehicle applications in which the fan is located in front of the radiator. Together with the increasing computational power of the computers, the current computational model may also be implemented for the under hood domain simulations of the complete cooling system.

REFERENCES

[1] T. Birch, "Automotive Heating and Air Conditioning*", 4th Ed., Pearson Prentice Hall,* 2006.

[2] A. Bejan, D. A. Nield, "Convection in Porous Media", *3rd Ed., Springer,* 2006

[3] "Fluent 14.5 Theory Guide" *ANSYS Inc, vol. 5,* 2013

[4] K. H. Do, J. Y. Min, S. J. Kim, "Thermal Optimization of an Internally Finned Tube Using Analytical Solutions Based on a Porous Medium Approach", *ASME, Journal of Heat Transfer, vol. 129,* 2007.

[5] S. J. Kim, D. Kim, "Forced Convection in Microstructures for Electronic Equipment Cooling", *ASME, Journal of Heat Transfer, vol. 121,* 1999.

[6] D. Kim, S. J. Kim, "Compact Modeling of Fluid flow and Heat Transfer in Straight Fin Heat Sinks", *ASME, Journal of Electronic Packaging, vol. 126,* 2004.

[7] T. Jeng and S. Tzeng, "A semi-empirical model for estimating permeability and inertial coefficient of pin-fin heat sinks", *International Journal of Heat and Mass transfer, vol. 48, 3140-3150,* 2005.

[8] T. Jeng, S. Tezeng, Y. Hung, "An analytical study of local thermal equilibrium in porous heat sinks using fin theory", *International Journal of Heat and Mass Transfer, vol. 49, 1907-1914,* 2006.

[9] F. P. Incropera, D. P. DeWitt, T. L. Bergman, A. S. Lavine, "Fundamentals of Heat and Mass Transfer", *6th Ed., Wiley,* 2007.

[10] N. Kulasekharan, H. R. Purushotham, G. C. Junjanna, "Performance improvement of a louver-finned automobile radiator using conjugate thermal CFD analysis", *International Journal of Engineering Research & Technology, 2278-0181, vol. 1 issue 8,* 2012.

[11] M. Y. Wen, C. Y. Ho, "Heat transfer enhancement in fin and tube heat exchanger with improved fin design", *Applied Thermal Engineering, vol. 29, pp 1050-1057,* 2009.

[12] W. M. Yan, P. J. Sheen, “Heat transfer and friction characteristics of fin and tube heat exchangers”, *International Journal of Heat and mass transfer, vol. 43, pp 1651-1659,* 2000.

[13] L. Sheik Ismail, C. Ranganatakului Ramesh K. Shah, “Numerical Study of Flow Patterns of Compact Plate-fin Heat Exchangers and Generation Design Data for Offset and Wavy Fins”, *International Journal of Heat and Mass Transfer, vol. 52, pp. 3972 – 3983,* 2009.

[14] N. C. DeJong, L. W. Zhang, A. M. Jacobi, S. Balachandar, D. K. Tafti, “A complementary Experimental and Numerical Study of the Flow and Heat Transfer in Offset Strip-Fin Heat Exchangers”, *ASME, Journal of Heat Transfer, vol. 120,* 1998.

[15] H. You, C. H. Chang, “Determination of flow properties in non-darcian flow”, *ASME, Journal of Heat Transfer, vol. 119, 190-192,* 1997.

[16] A. Zukauskas, A. Ulinskas, “Efficiency parameters for heat transfer in tube banks”, *Heat Transfer Engineering, vol. 6, 19-25,* 1985.

[17] Y. Varol, H. Öztop, A. Varol, “Effects of Thin Fin on Natural Convection in Porous Triangular Enclosures”, I*nternational Journal of Thermal Sciences, pp. 1033–1045,* 2007.

[18] J.Yang, M. Zeng, Q. Wang, “Forced Convection Heat Transfer by Porous Pin Fins in Rectangular Channels”, *Quiwang Wang, vol. 132,* May 2010.

[19] S. Jain, Y. Deshpande, “CFD Modeling of a Radiator Axial Fan for Air Flow Distribution”, *World Academy of Science, Engineering and Technology, vol. 71,* 2012.

[20] Z. Zhang, Y. Li, “CFD simulation on inlet configuration of plate-fin heat exchangers”, *Cryogenics, vol. 43, 673-678,* 2003.

[21] K. L. Wasewar, S. Hargunami, P. Atluri, N. Kumar, “CFD Simulation of Flow Distribution in the Header of Plate-Fin Heat Exchangers”, *Chem. Eng. Technol., vol. 30, no. 10, 1340-1346,* 2007.

[22] B. R. Baliga, R. R. Azrak, “Laminar Fully Developed Flow and Heat Transfer in Triangular Plate-Fin Ducts”, *ASME, Journal of Heat Transfer , vol. 108,* 1986.

[23] L. Zangh, “Laminar flow and heat transfer in plate-fin triangular ducts in thermally developing entry region”, *International Journal of Heat and Mass Transfer, vol. 50, 1637-1640,* 2007.

[24] C. Oliet, J. Castro, C.D. Perez-Segarra, "Parametric Studies on Automotive Radiators", *Applied Thermal Engineering, vol. 27, pp. 2033 – 2043,* 2009.

[25] Li-Zhi Zhang, "Flow Maldistribution and Thermal Performance Deterioration in a Cross-Flow Air to Air Heat Exchanger with Plate-Fin Cores", *International Journal of Heat and Mass Transfer, vol. 52, pp. 4500 – 4509,* 2009.

[26] A.Hayes, J. Khan, A. Shaaban, I. Spoearing, "The Thermal Modeling of a Matrix Heat Exchanger Using a Porous Medium and the Thermal Non-Equilibrium Model", *International Journal of Thermal Sciences, vol. 47, pp. 1306 – 1315,* 2008.

[27] S. Mao, C. Cheng, X. Li, Efsathios E. Michaelides, "Thermal/Structural Analysis of Radiators for Heavy-duty Trucks", *Applied Thermal Engineering, vol. 30, pp. 1438 – 1446,* 2010.

[28] T. Ogushi, H. Chiba, H. Nakajima, "Development of Lotus-Type Porous Heat Sink", *Materials Transactions, vol. 47, No. 9, pp. 2240 – 2247,* 2006.

[29] E. Carluccio, G. Starace, A. Ficarella, D. Laforgia, "Numerical Analysis of a Cross-Flow Compact Heat Exchanger for Vehicle Applications", *Applied Thermal Engineering, vol. 25, pp. 1995 – 2013,* 2005.

[30] W. Wang, J. Guo, S. Zhang, J. Yang, X. Ding, X. Zhan, "Numerical Study on Hydrodynamic Characteristics of Plate-fin Heat Exchanger Using Porous Media Approach", *Computers and Chemical Engineering, vol. 61, pp. 30 – 37,* 2014.

[31] B. I. Pavel, A. A. Mohamad, "An experimental and numerical study on heat transfer enhancement for gas heat exchangers fitted with porous media", *International Journal of Heat and Mass Transfer, vol. 47, 4939-4952,* 2004.

[32] Q. Yu, A. G. Straatman, B. E. Thompson, "Carbon-foam finned tubes in air-water heat exchangers", *Applied Thermal Engineering, vol. 26, 131-143,* 2006.

[33] E. Aydar, İ. Ekmekçi, "Thermal Efficiency Estimation of the Panel Type Radiators with CFD Analysis", *Journal of Thermal Science and Technology, vol. 63, 63-71,* 2012.

[34] V. Gullapallı, B. Sundén, "CFD Simulation of Heat Transfer and Pressure Drop in Compact Brazed Heat Exchangers", *Heat Transfer Engineering, vol. 35 (4), 358-366,* 2014.

[35] D. Taler, “Experimental determination of correlations for average heat transfer coefficients in heat exchangers on both fluid sides”, *Heat and Mass Transfer, vol. 49, 1125-1139,* 2013.

[36] W. M. Yang, S. K. Chou, K. J. Chua, J. Li, X. Zhao, “Research on modular micro combustor-radiator with and without porous media”, *Chemical Engineering Journal, vol. 168, 799-802,* 2011.

[37] P. Jiang, M. Fan, G. Si, Z. Ren, “Thermal-hydraulic performance of small scale micro-channel and porous-media heat-exchangers”, *International Journal of Heat and Mass Transfer, vol. 44, 1039-1051,* 2001.

[38] M. H. Aksel, “Notes on Fluid Mechanics*”, Metu press, vol. 1-2,* 2008.